Constraints on Nuclear EOS by Nuclear Response Experiments

Atsushi Tamii

Research Center for Nuclear Physics (RCNP)
Osaka University, Japan

from the studies with the Grand Raiden spectrometer at RCNP

Physics of Core-Collapse Supernova and Compact Star Formations
March 19-21, 2018, Waseda University

Nuclei as a Micro-Physics Laboratory

Study of nuclear properties

- Systematic properties of nuclei and nuclear matter
- Properties of individual nuclides, excited states, and reactions

Experimental Methods

- Stable nuclei (target): higher resolution, statistics, and accuracy
- Unstable nuclei (beam): exotic nuclei, broader systematics

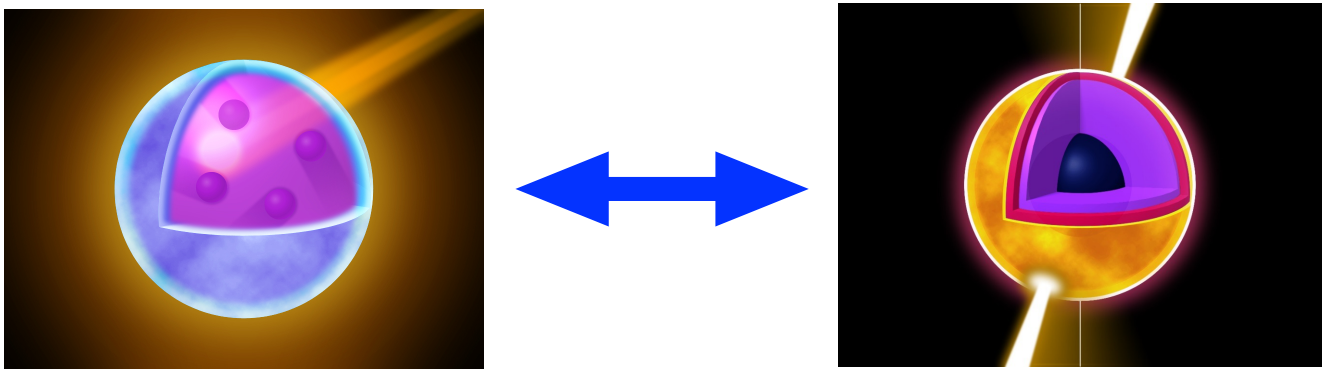

Nucleus Neutron Star

Strategy

I will focuses on the properties of the nuclear matter in the conditions of

$N \gtrsim Z$	→	*neutron matter*
$\rho \sim \rho_0$	→	*high density*
$T = 0$	→	*finite temperature*
p and n	→	*strangeness*

Ordinary nuclear matter

Starting point for the studies of the more exotic conditions

Strategy

High-quality data of nuclear responses

e.g. electric dipole response

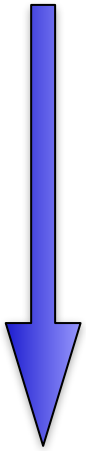

Theoretical models

Mean-field models

Parameters of the nuclear equation of states

e.g. J and L

Nuclear EOS

is important for nuclear physics and nuclear-astrophysics

Core-collapse supernova

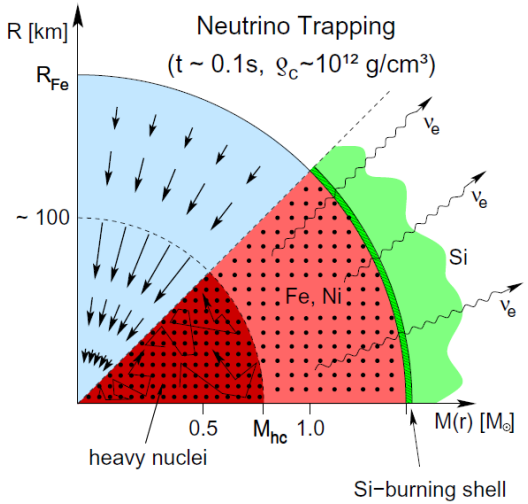

Langanke and Martinez-Pinedo

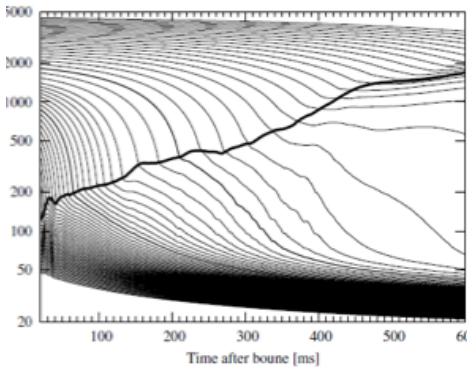

Y. Suwa et al., ApJ764, 99 (2013).

Nucleosynthesis

Neutron star mass vs radius

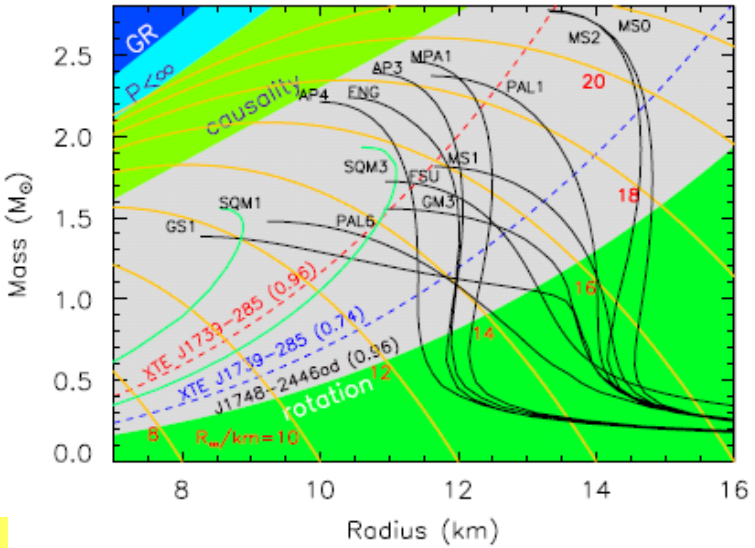

Lattimer et al., Phys. Rep. 442, 109(2007)

Neutron Star Merger Gravitational Wave

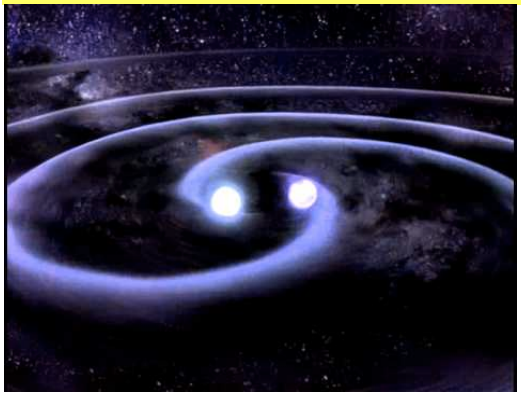

https://www.youtube.com/watch?v=IZhNWh_lFuI

Neutron star cooling

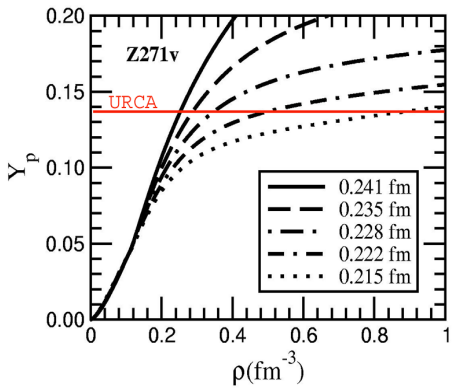

Lattimer and Prakash, Science 304, 536 (2004).

Neutron star structure

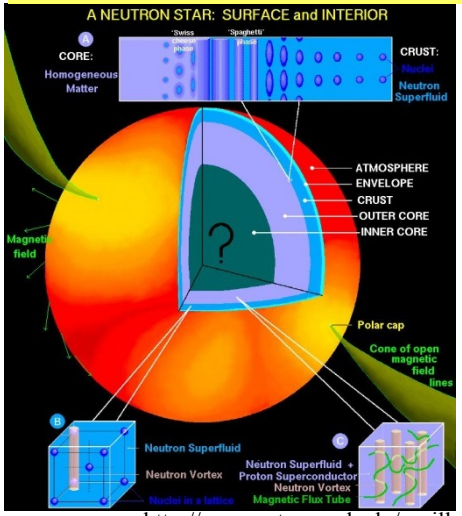

http://www.astro.umd.edu/~miller/nstar.html

Nuclear Equation of State (EOS)
at zero temperature

Nuclear EOS neglecting Coulomb

$$\frac{E}{A}(\rho,\delta)=\frac{E}{A}(\rho,0)+S(\rho)\delta^2+\cdots$$

$$\delta\equiv\frac{\rho_n-\rho_p}{\rho_n+\rho_p}$$ Asymmetry parameter

Symmetry energy

$$S(\rho)=J+\frac{L}{3\rho_0}(\rho-\rho_0)+\ldots$$

⇔ difference between *p*-*n* chemical potentials: how the system energy changes when protons are replaced by the neutrons

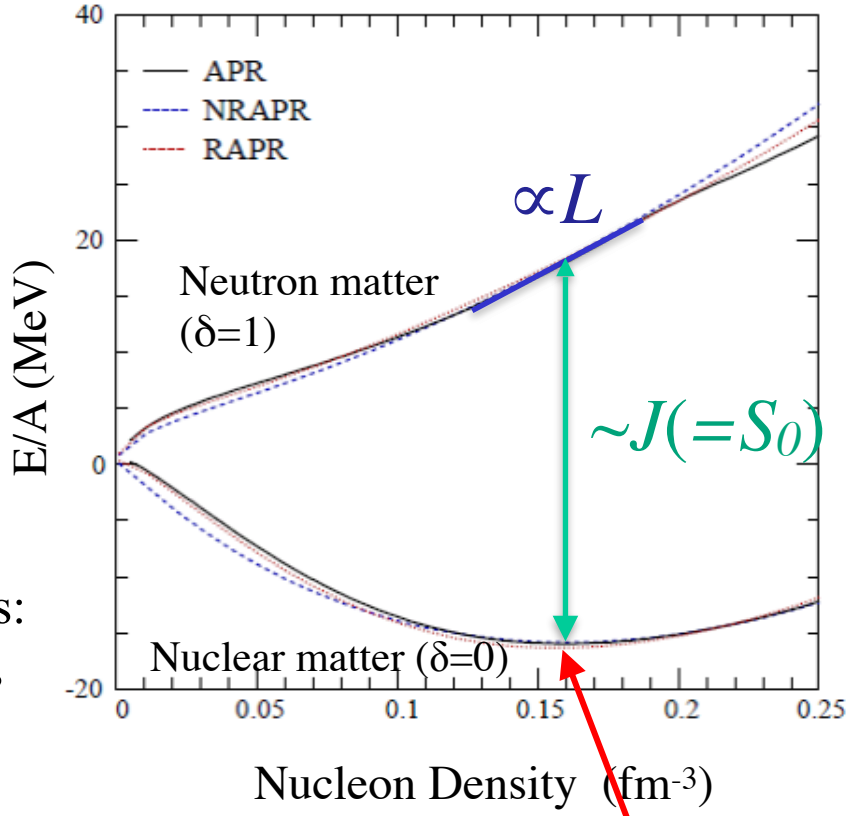

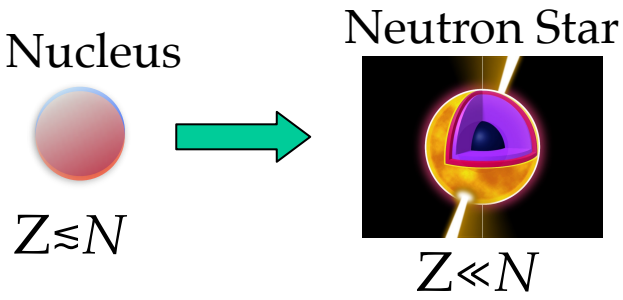

Electric Dipole Response of Nuclei and the Nuclear Symmetry Energy

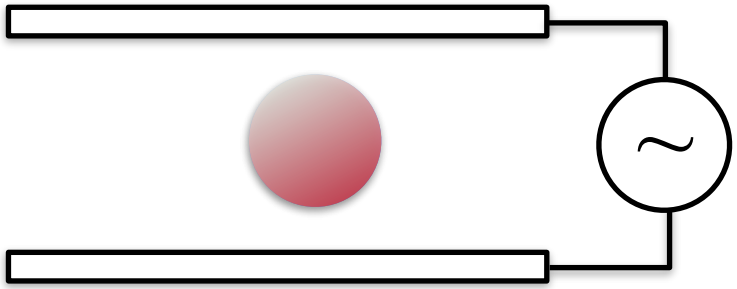

Nuclear Equation of State: How?

How can we study the EOS?

Thermodynamics

Give a "small perturbation" to the system

then observe how the system changes

→ responses

$$\kappa = -\frac{1}{V}\left(\frac{dV}{dp}\right)_S$$ adiabatic compressibility

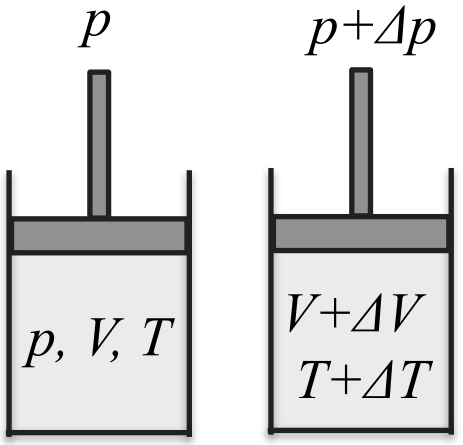

equilibrium

Nuclear EOS

Give a small perturbation by an external field

then observe how the system changes

→ nuclear responses

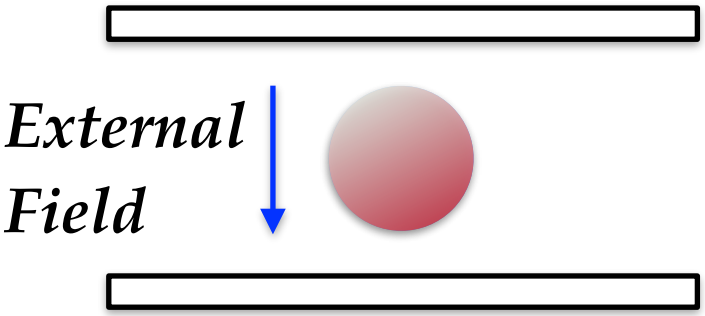

EDP is determined from the photo-absorption cross sections

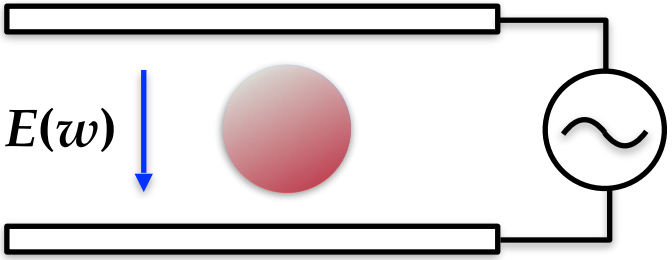

dielectric material
in an oscillating electric field

EDP is determined from the photo-absorption cross sections

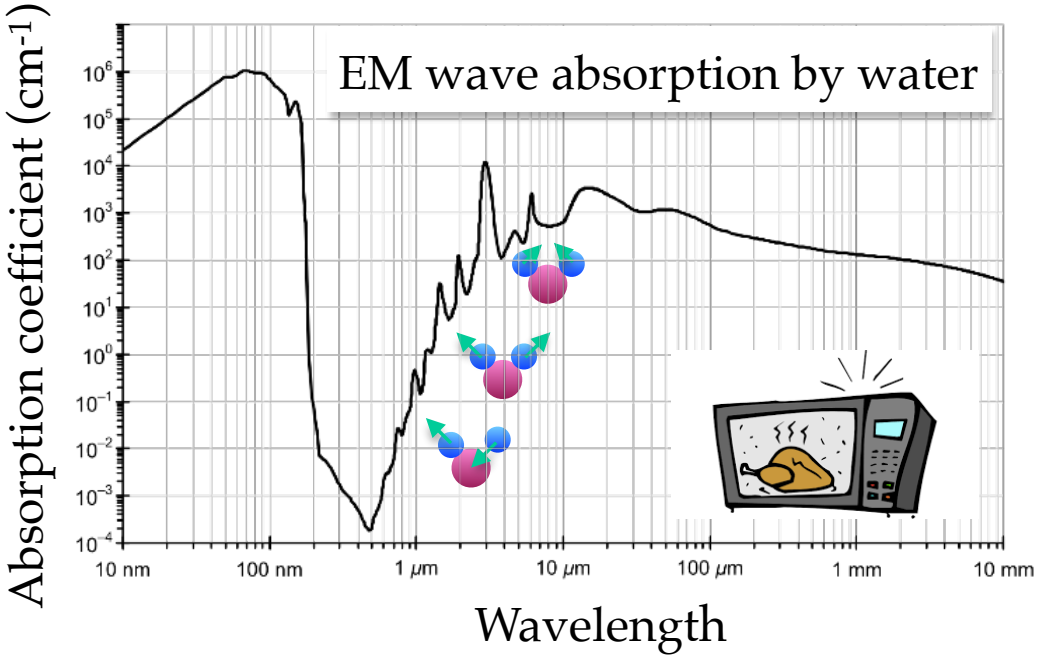

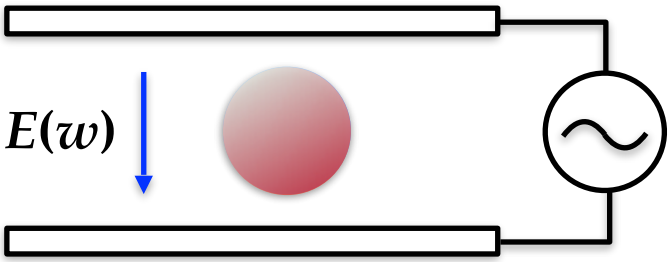

dielectric material
in an oscillating electric field

EDP is determined from the photo-absorption cross sections

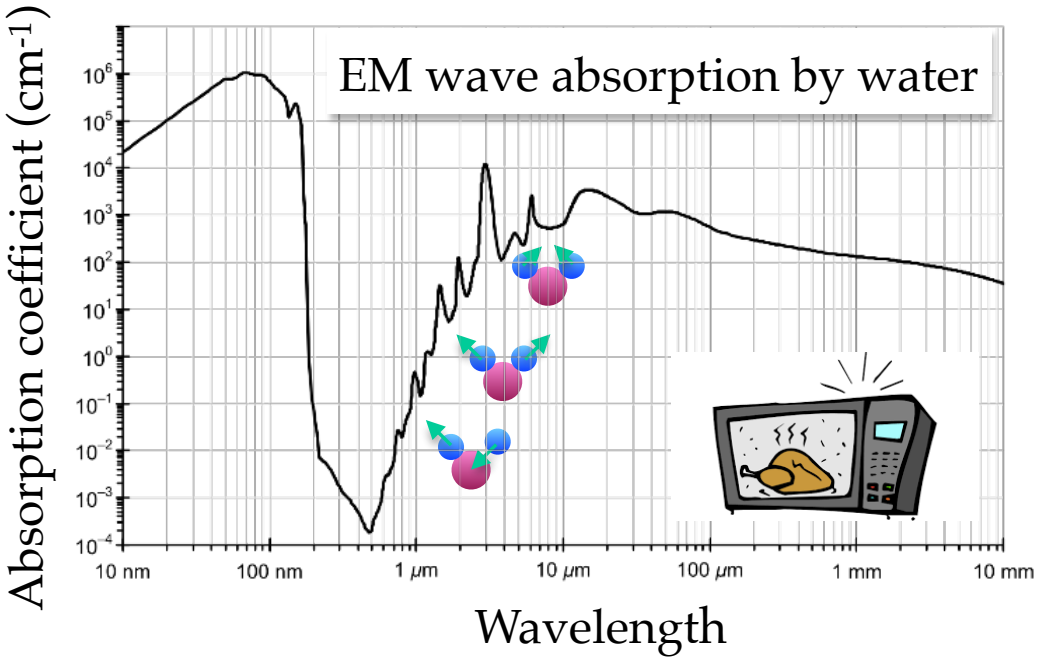

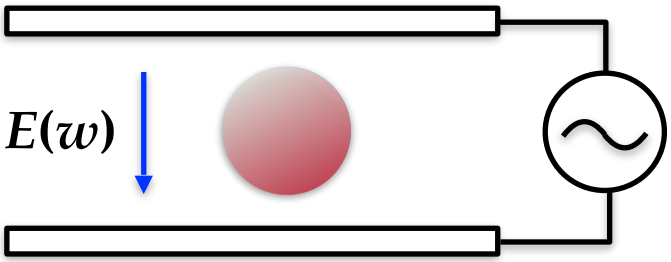

dielectric material
in an oscillating electric field

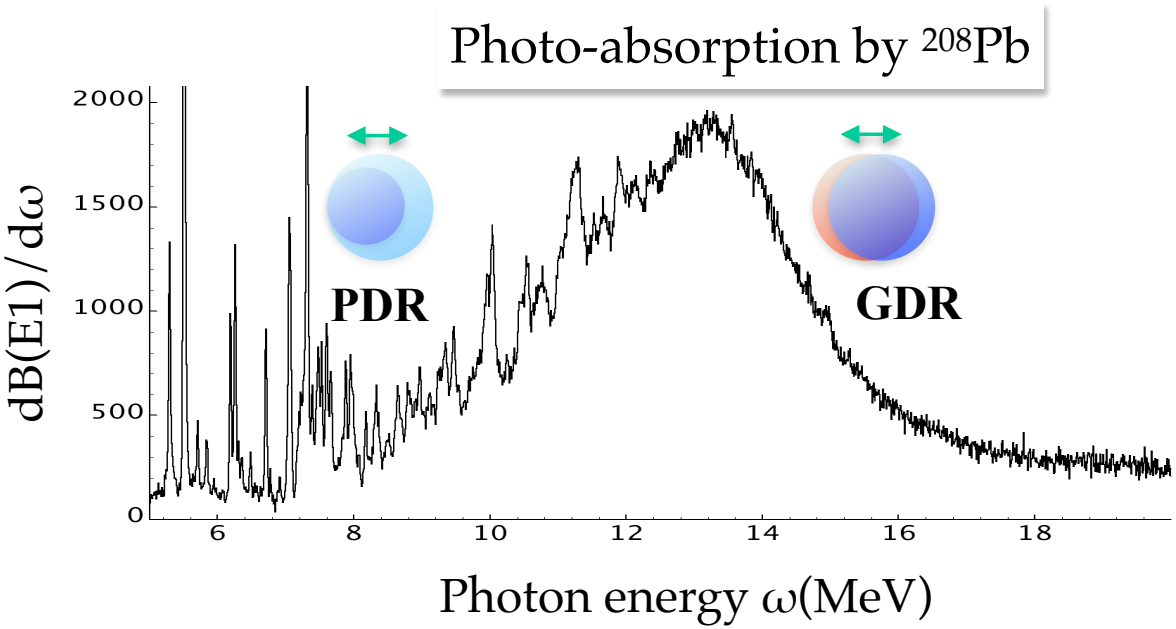

EDP is determined from the photo-absorption cross sections

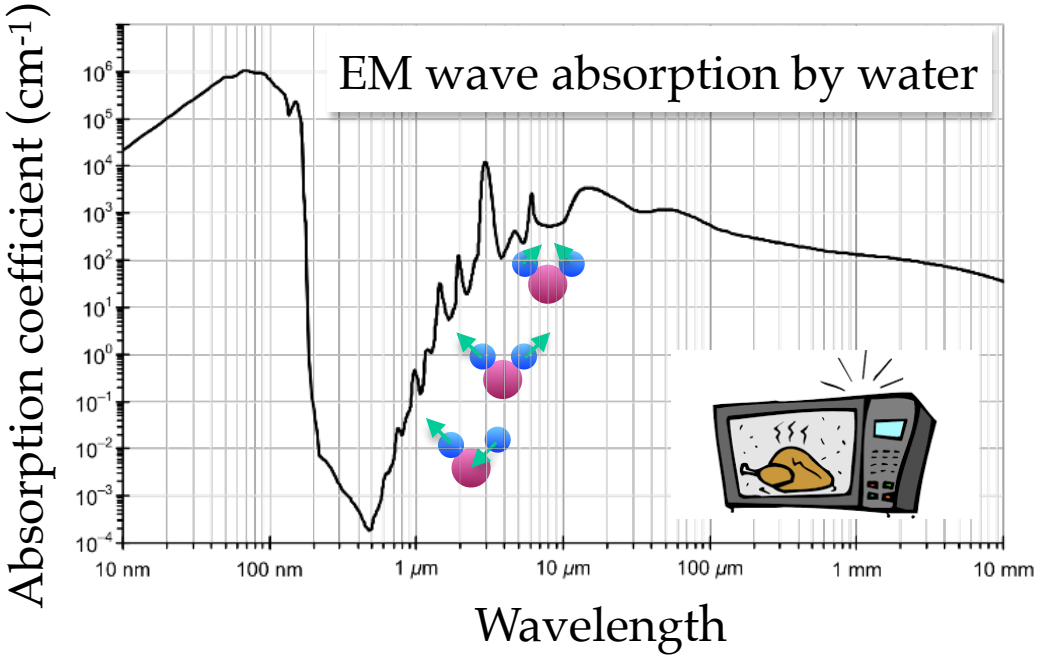

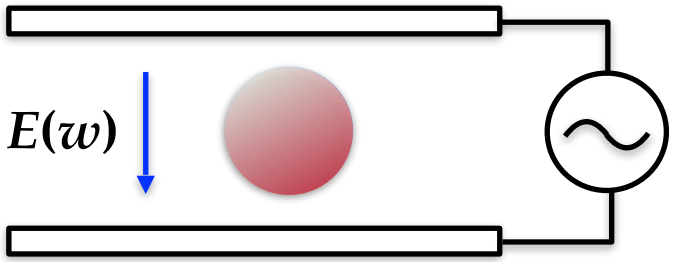

dielectric material
in an oscillating electric field

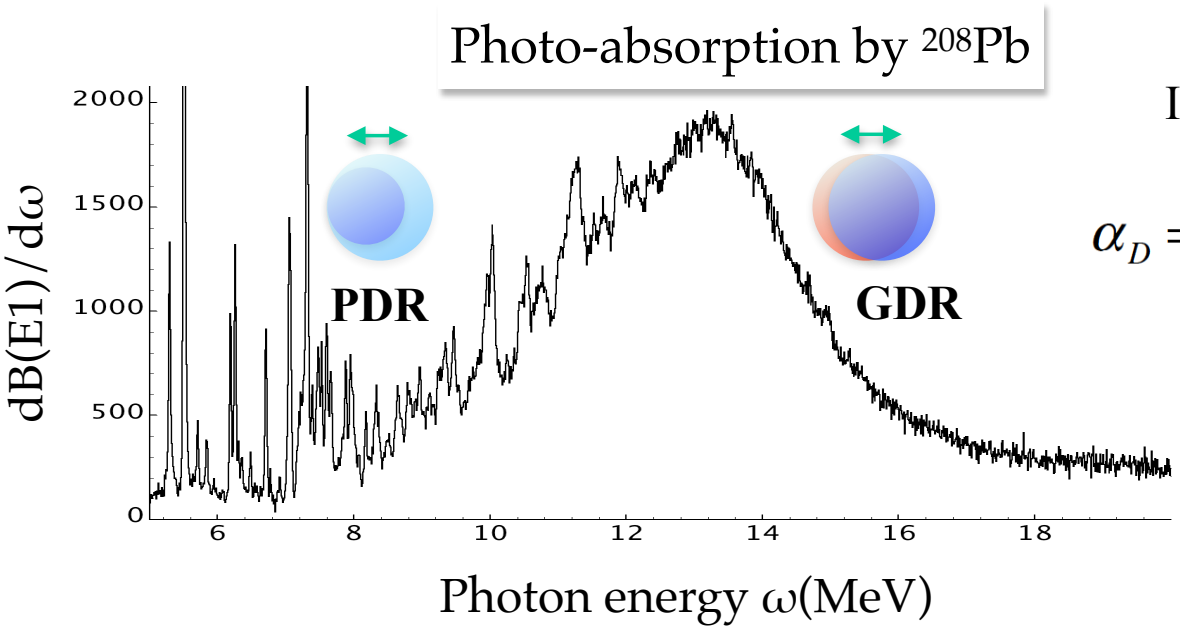

Inversely energy-weighted sum-rule

$$\alpha_D = \frac{\hbar c}{2\pi^2}\int \frac{\sigma_{\mathrm{abs}}^{E1}}{\omega^2} d\omega = \frac{8\pi}{9}\int \frac{dB(E1)}{\omega}$$

first order perturbation calc.

A.B. Migdal: 1944

Electric Dipole Polarizability (α_D)

Electric dipole moment

$$p = \alpha_D \times E$$

α_D: electric dipole polarizability

The **restoring force** originates from the **symmetry energy.**

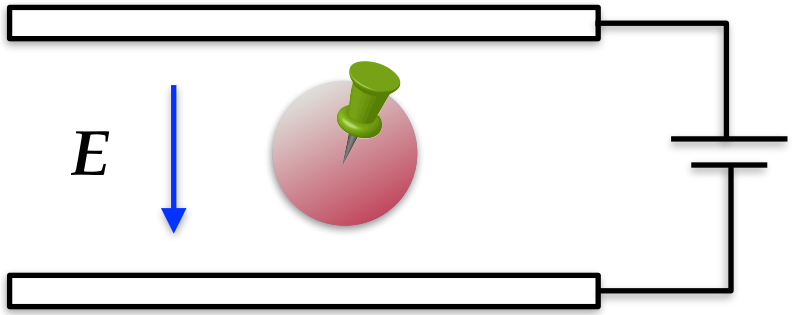

nucleus
in a static electric field
with fixing the c.m. position

Inversely energy-weighted sum-rule of B(E1)

$$\alpha_D = \int \frac{1}{\omega} \frac{dB(E1)}{d\omega} d\omega$$

first order perturbation calc.

A.B. Migdal: 1944

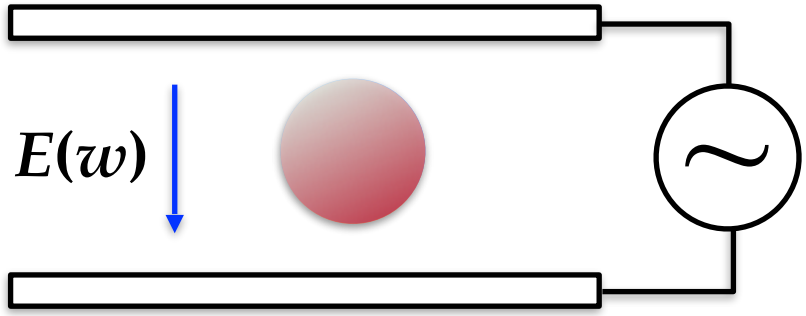

dielectric material
in an oscillating electric field

Electric Dipole Polarizability (α_D)

Electric dipole moment

$$p = \alpha_D \times E$$

α_D: electric dipole polarizability

The **restoring force** originates from the **symmetry energy.**

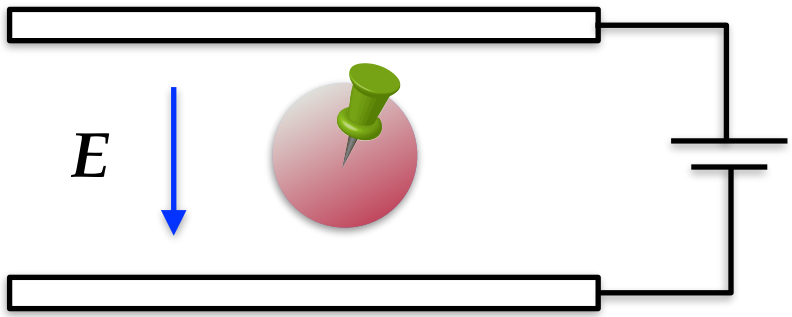

nucleus
in a static electric field
with fixing the c.m. position

Electric Dipole Polarizability (α_D)

Electric dipole moment

$$p = \alpha_D \times E$$

α_D: electric dipole polarizability

The **restoring force** originates from the **symmetry energy.**

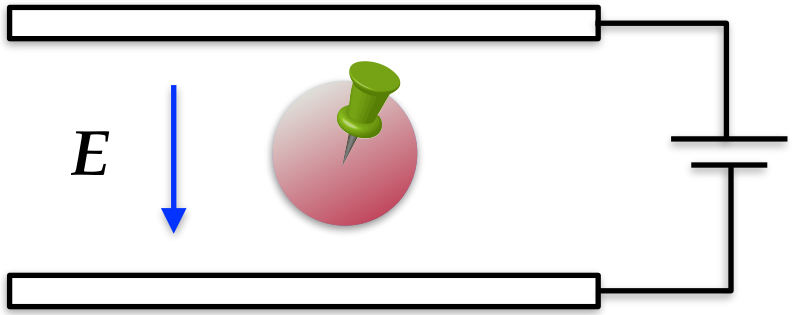

nucleus
in a static electric field
with fixing the c.m. position

Inversely energy-weighted sum-rule of B(E1)

$$\alpha_D = \int \frac{1}{\omega} \frac{dB(E1)}{d\omega} d\omega$$

first order perturbation calc.

A.B. Migdal: 1944

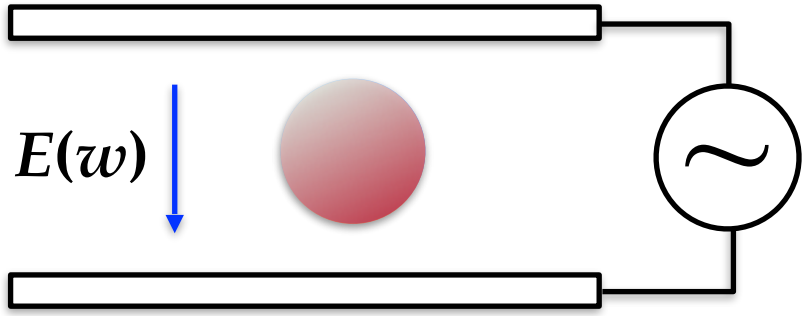

dielectric material
in an oscillating electric field

Electric Dipole Polarizability (α_D) in the correlation of J and L

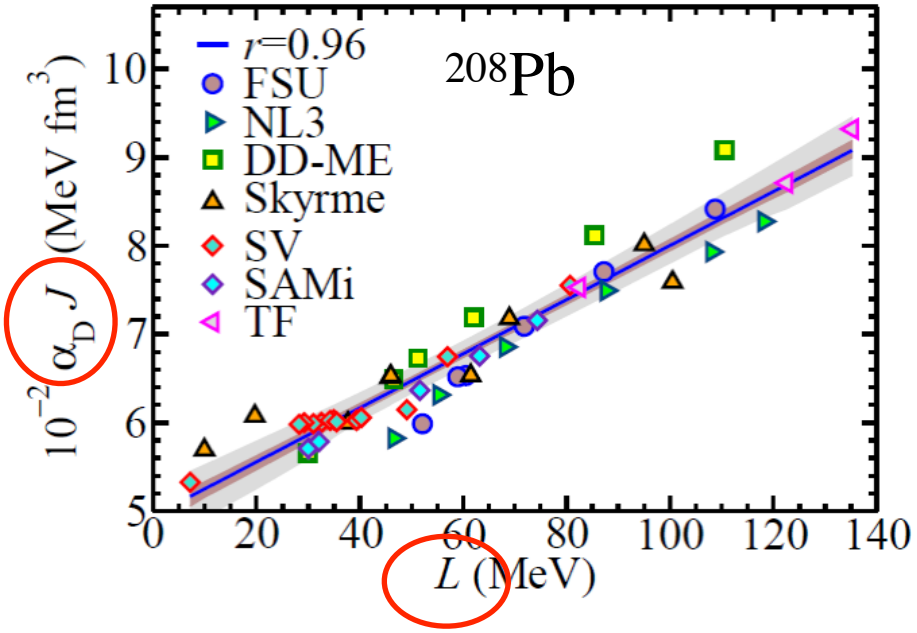

X. Roca-Maza *et al.*, PRC**88**, 024316(2013)

Correlations observed in various interaction sets in the framework of EDF.

$$\alpha_D^{\mathrm{DM}} \approx \frac{\pi e^2}{54}\frac{A\langle r^2\rangle}{J}\left[1+\frac{5}{3}\frac{L}{J}\epsilon_A\right]$$

insights from the droplet model

Precise determination of α_D of ^{208}Pb gives a constraint band in the *J*-*L* plane.

Electric Dipole Response of Nuclei

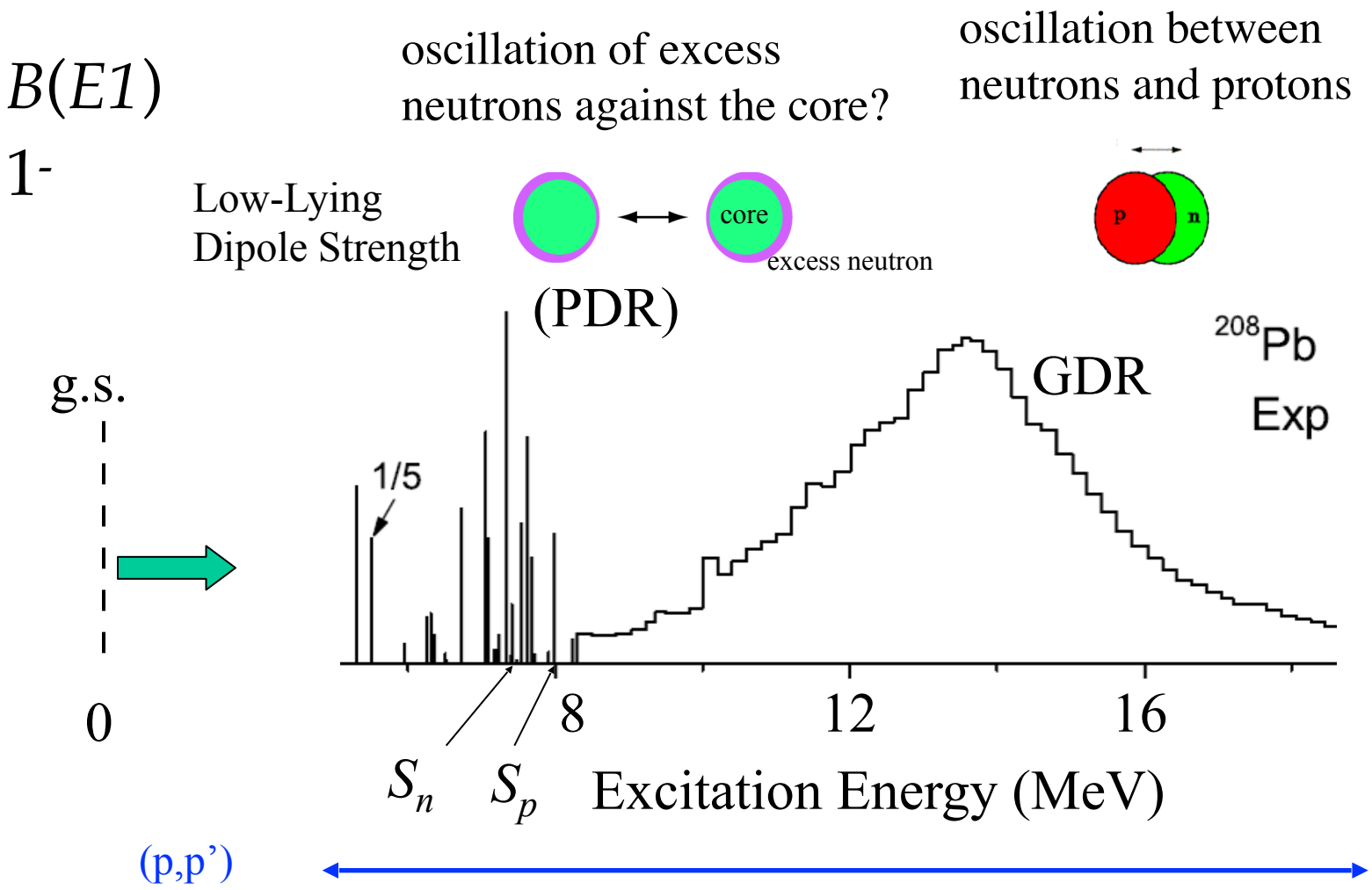

Probing the E1 Response by Proton Scattering

Missing Mass Spectroscopy by Virtual Photon Excitation

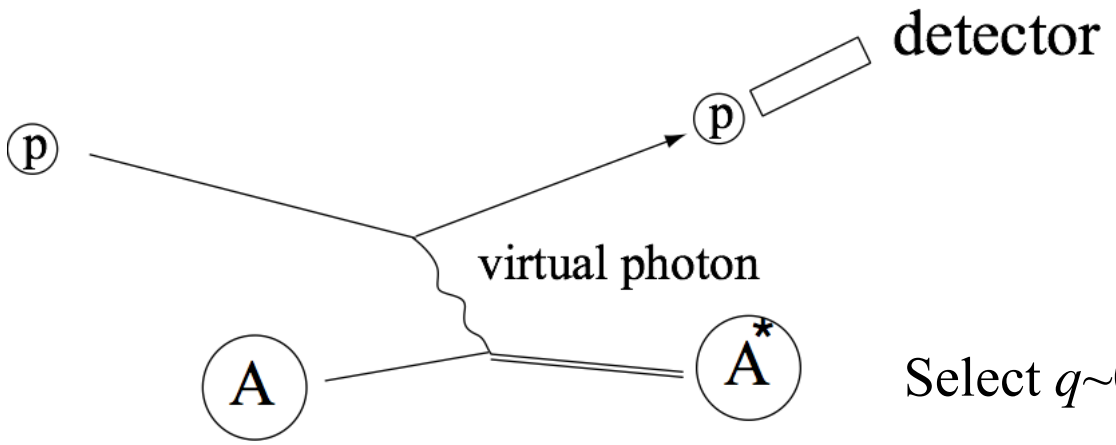

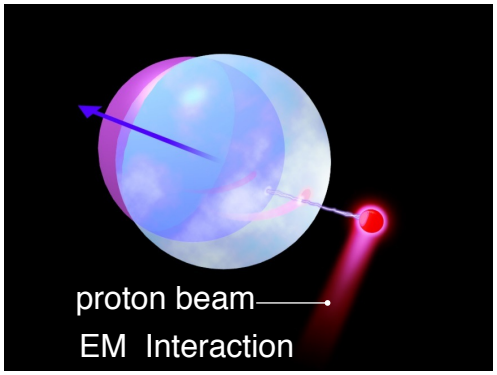

Select q~0 (~0 deg.)

- **Missing mass spectroscopy**:
  Total strength is measured independently from the decaying channels.
- **Multipole decomposition** of the strength in the continuum:
  Includes the contribution of unresolved small states
- **Coulomb excitation**: EM Interaction
  Absolute determination of the transition strength.

Neutron Skin and Density Dependence of the Symmetry Energy

Density distribution of protons and neutrons in a nucleus ^{208}Pb

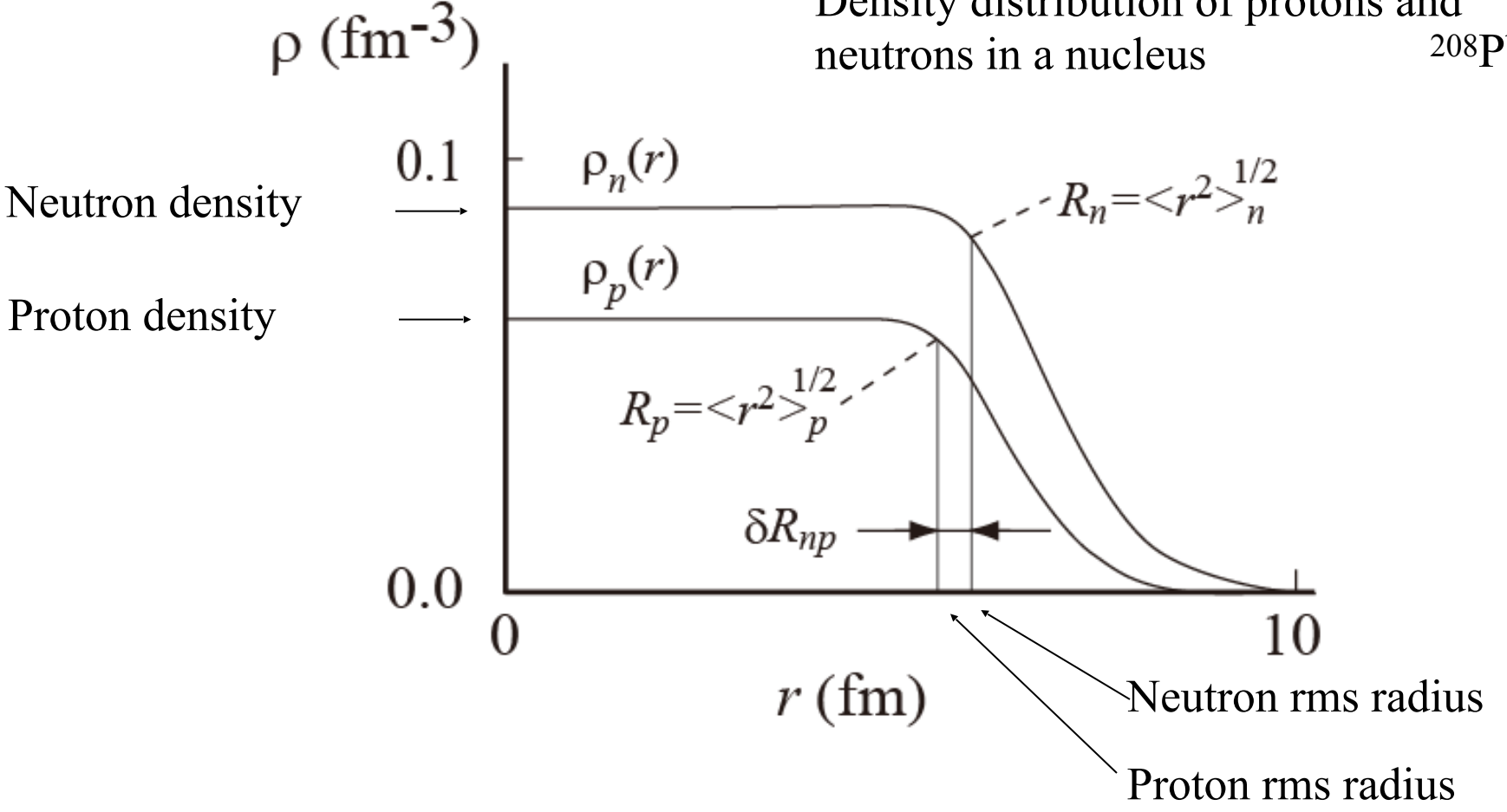

Neutron Skin and Density Dependence of the Symmetry Energy

For larger L:

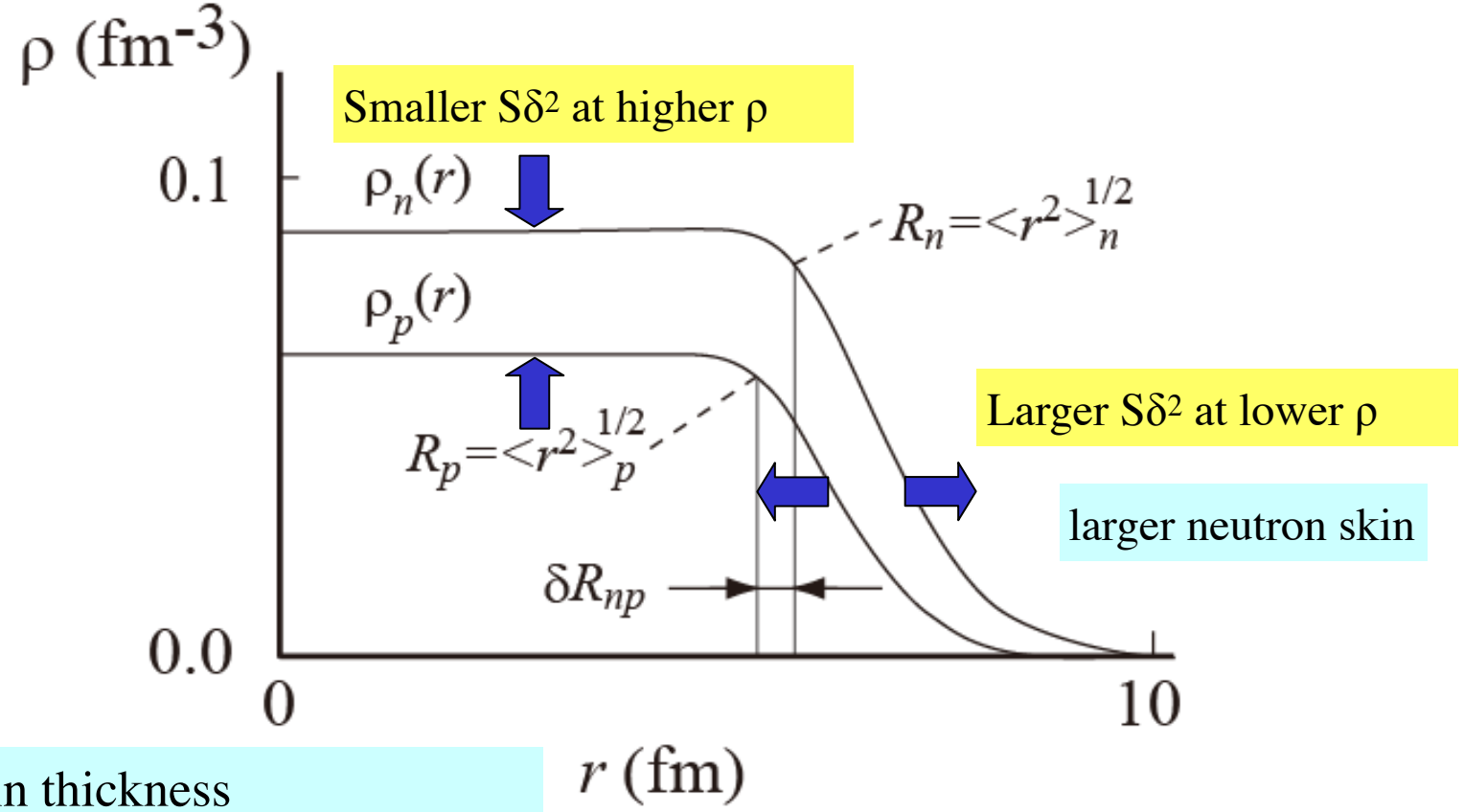

Neutron skin thickness

Density dependence of the symmetry energy

Energy minimum (equilibrium)

Neutron Skin and Density Dependence of the Symmetry Energy

For smaller L:

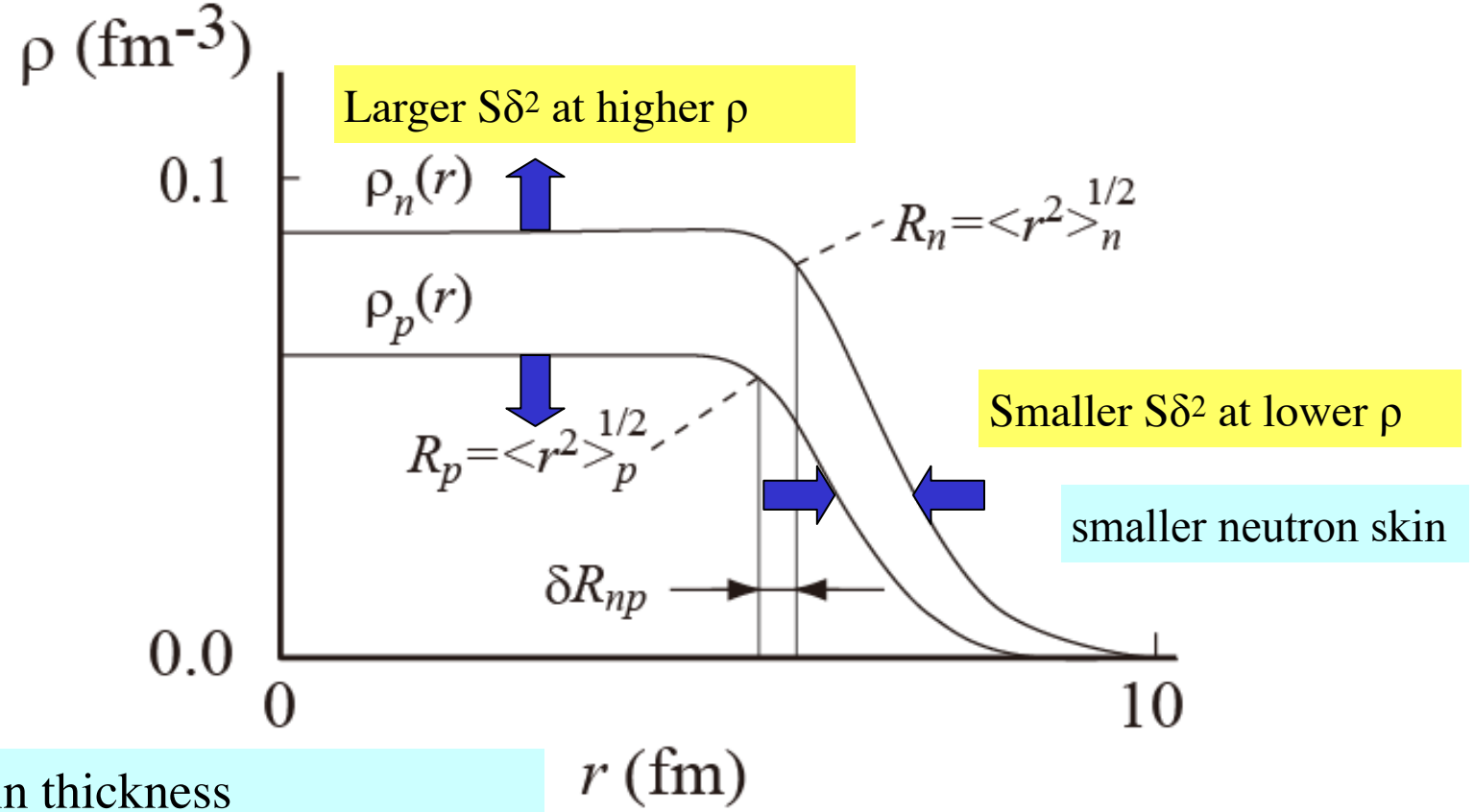

Neutron skin thickness

Density dependence of the symmetry energy

Energy minimum (equilibrium)

Neutron Skin and Density Dependence of the Symmetry Energy

X. Roca-Maza *et al.*, PRL**106**, 252501 (2011)

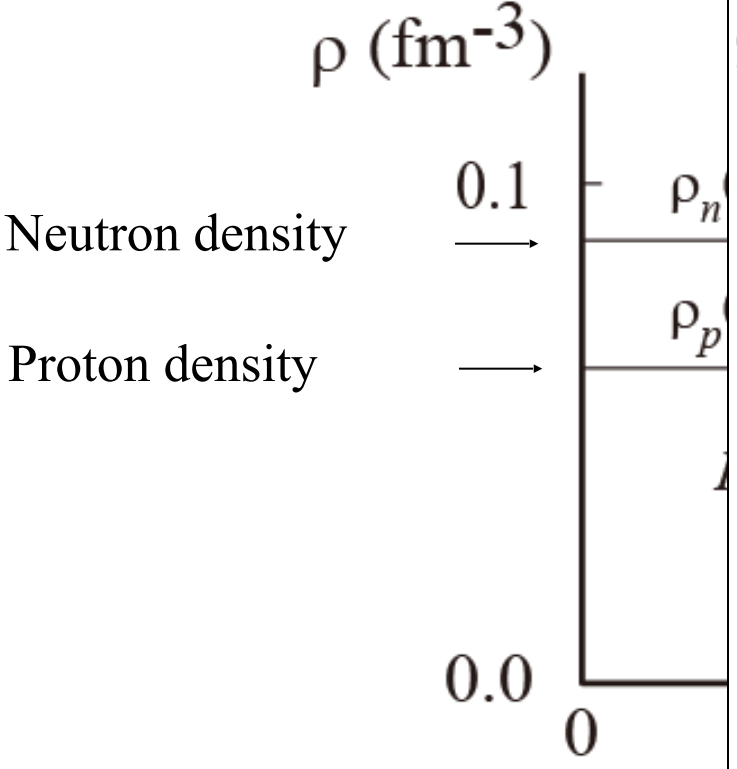

Neutron skin thickness

Density dependence of the symm

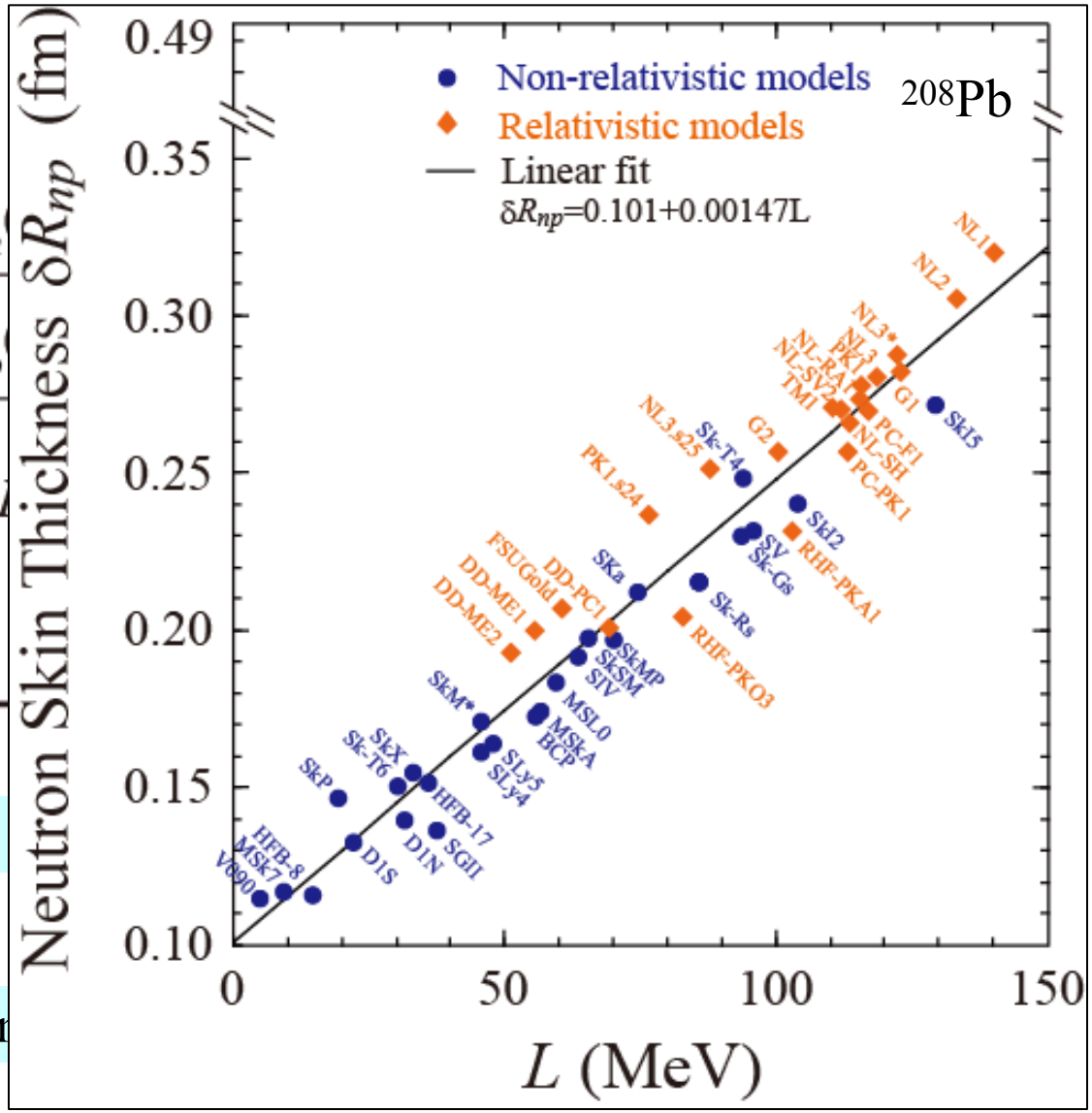

RCNP, Osaka Univ.


Tokyo
RCNP
OSAKA
~18 neutron stars

Research Center for Nuclear Physics (RCNP), Osaka University

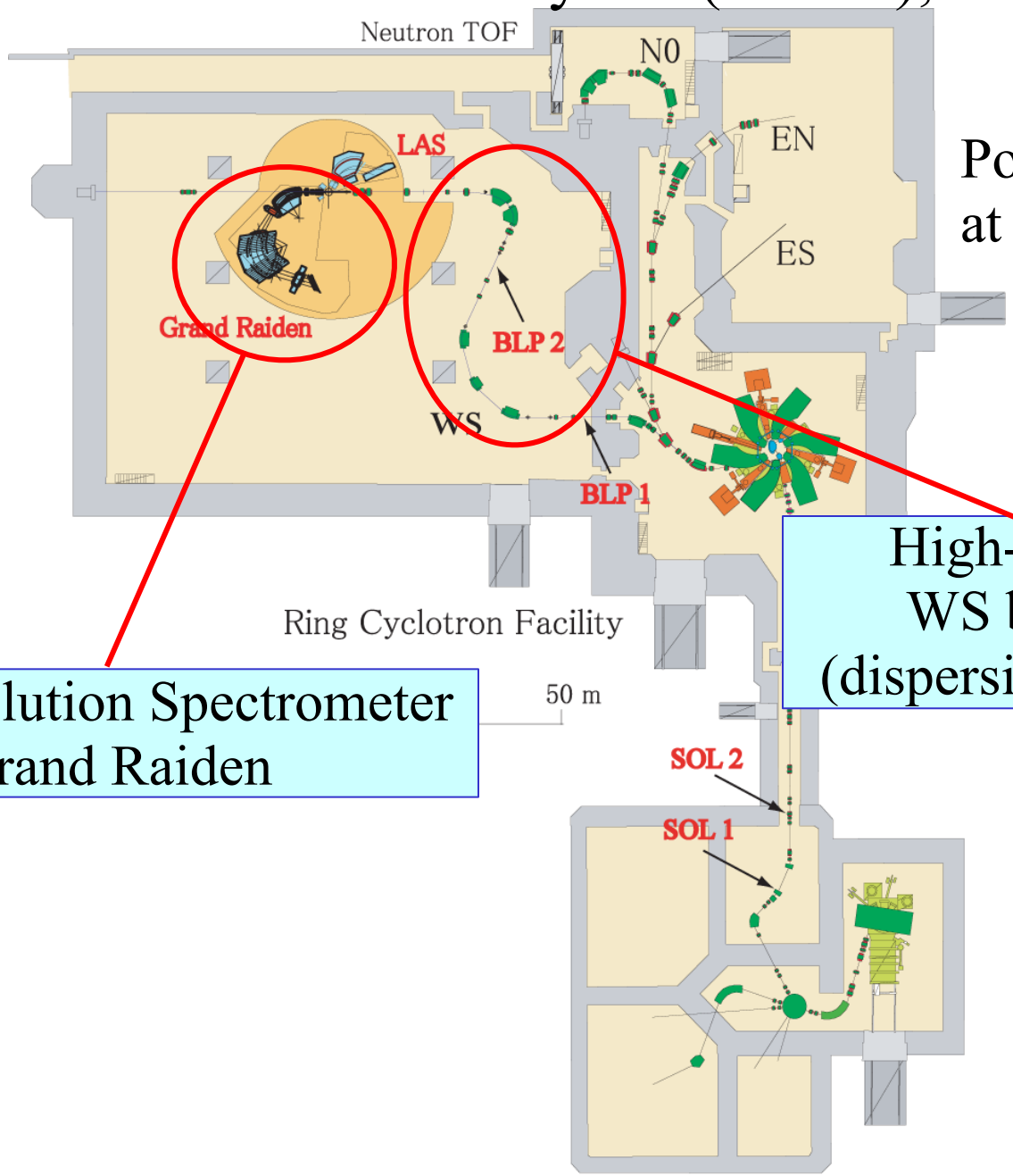

Polarized *p* beam
at 295 MeV

High-resolution
WS beam-line
(dispersion matching)

High-resolution Spectrometer
Grand Raiden

High-Resolution Spectrometer "Grand Raiden"

High resolution of 20-30 keV: dispersion matching.

Proton scattering
at very forward angles
at RCNP, Osaka Univ.

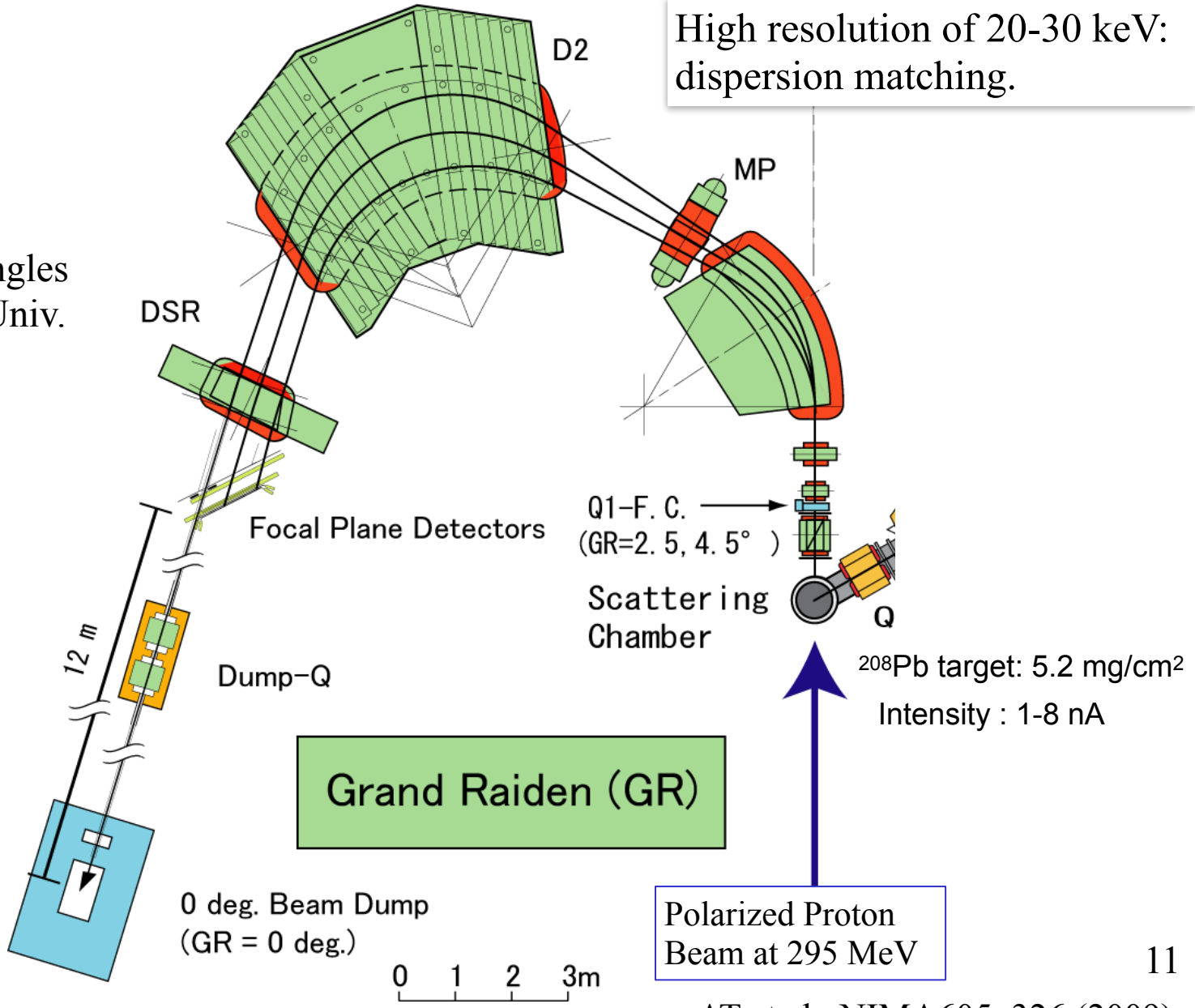

AT et al., NIMA605, 326 (2009)

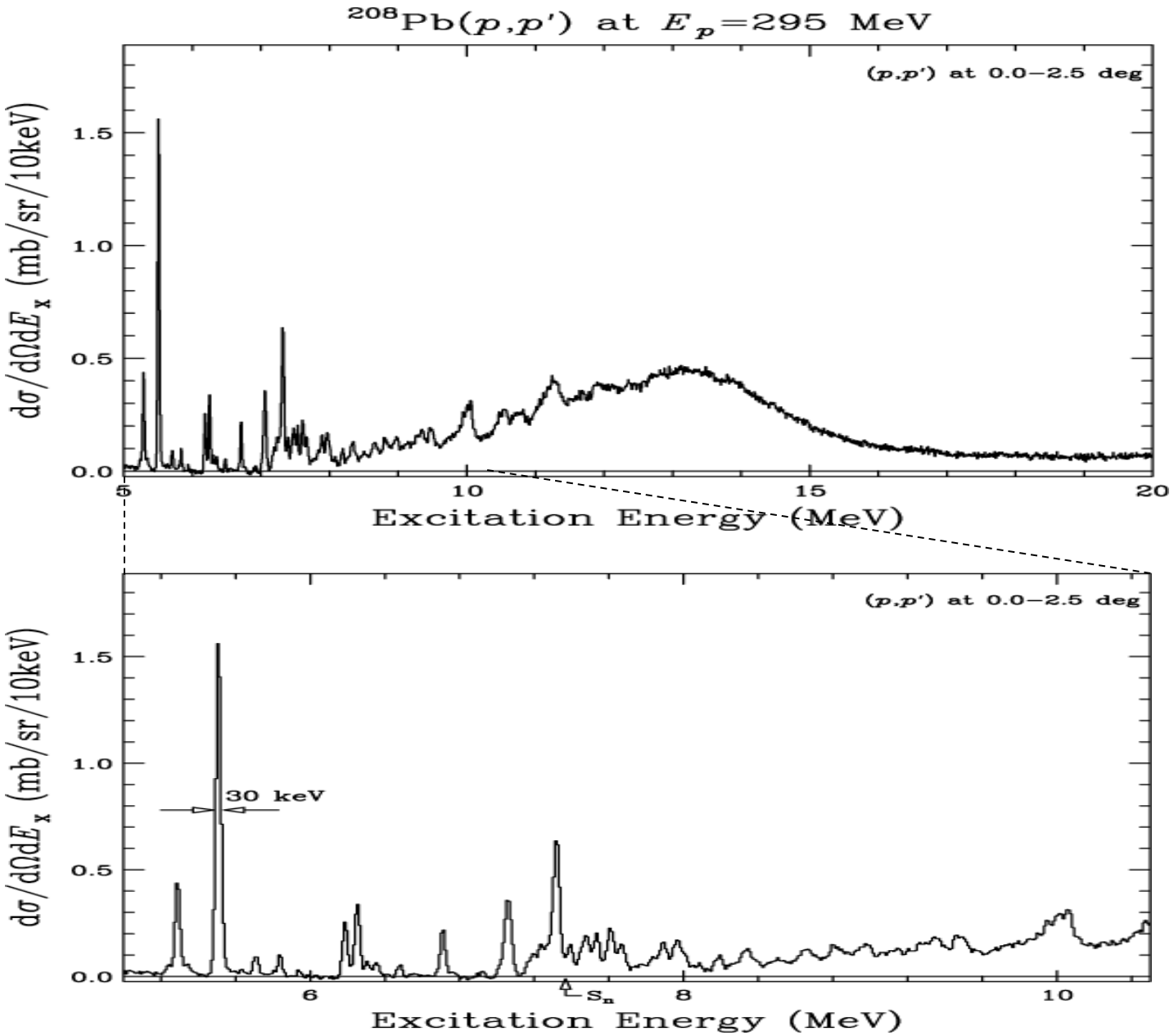
^{208}Pb(p,p′) at E_p=295 MeV
(p,p′) at 0.0−2.5 deg
dσ/dΩdE$_x$ (mb/sr/10keV)
Excitation Energy (MeV)
30 keV
S$_n$

B(E1): continuum and GDR region

Method 1: Multipole Decomposition

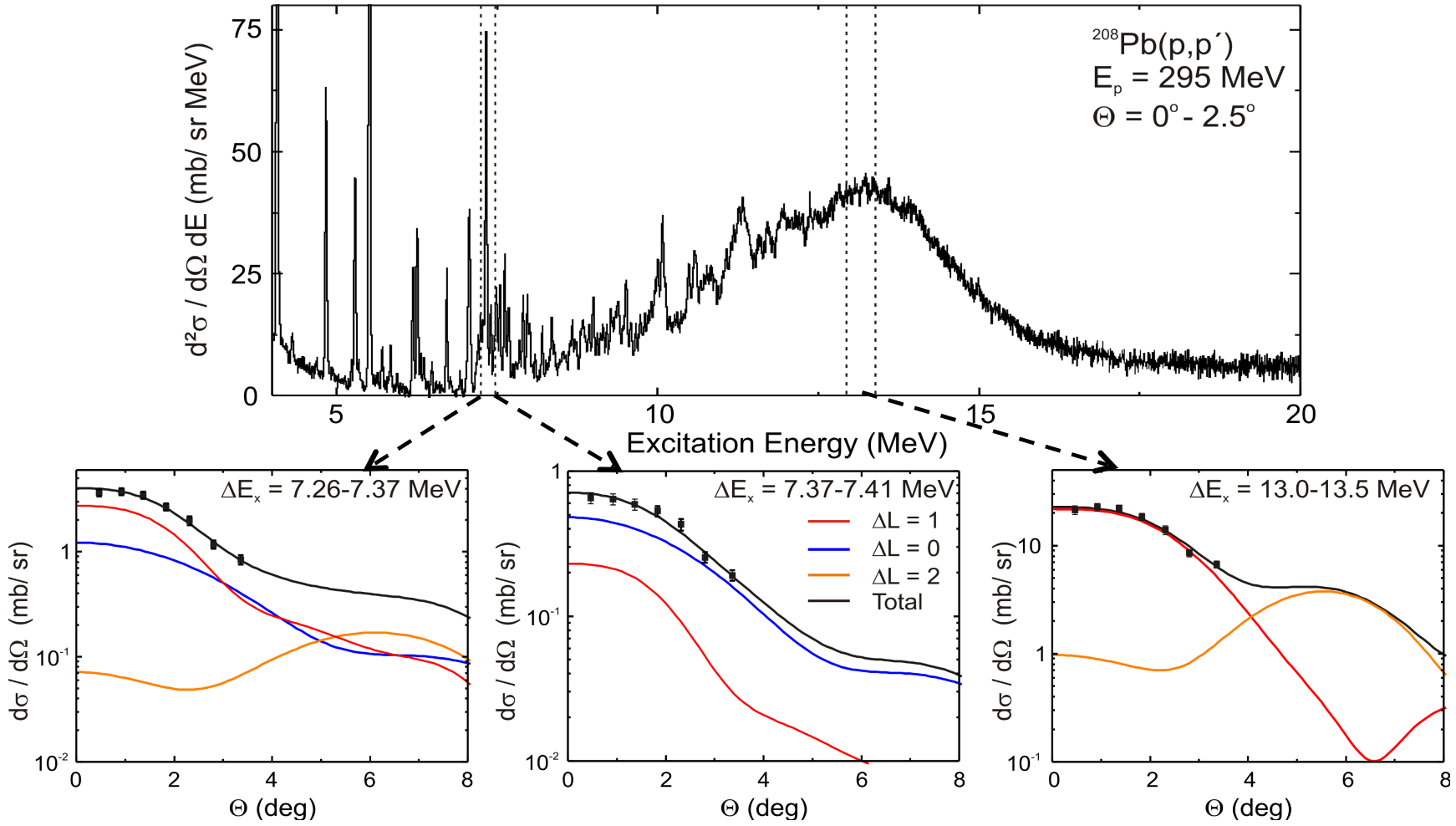

- Neglect of data for Θ>4: (p,p´) response too complex
- Included E1/M1/E2 or E1/M1/E3 (little difference)

Grazing Angle = 3.0 deg

B(E1): continuum and GDR region

Method 2: Decomposition by Spin Observables

- Polarization observables at 0° ➡ spinflip / non-spinflip separation
  model-independent
  T. Suzuki, PTP 103 (2000) 859

E1 / spin-M1 decomposition

$$\text{Total Spin Transfer } \Sigma \equiv \frac{3-(2D_{SS}+D_{LL})}{4} = \begin{cases} 1 \text{ for } \Delta S = 1 & \text{spin-M1} \\ 0 \text{ for } \Delta S = 0 & \text{E1} \end{cases}$$

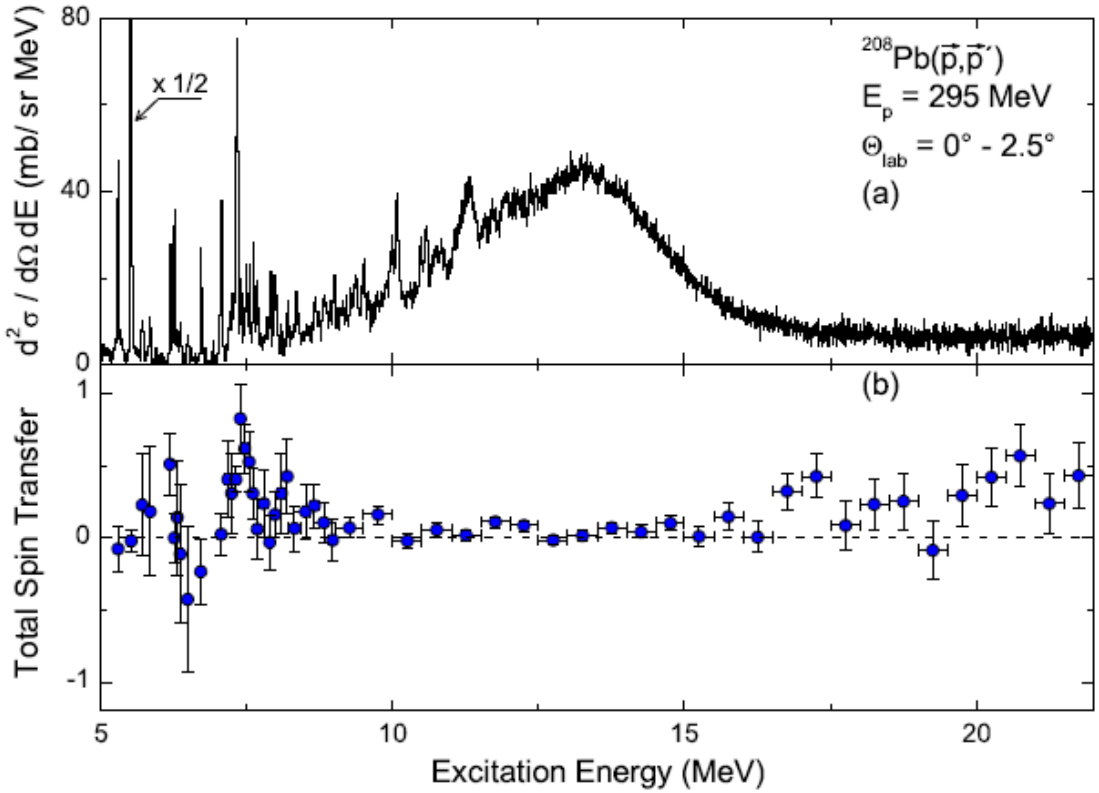

Electric Dipole Polarizability: ^{208}Pb, ^{120}Sn

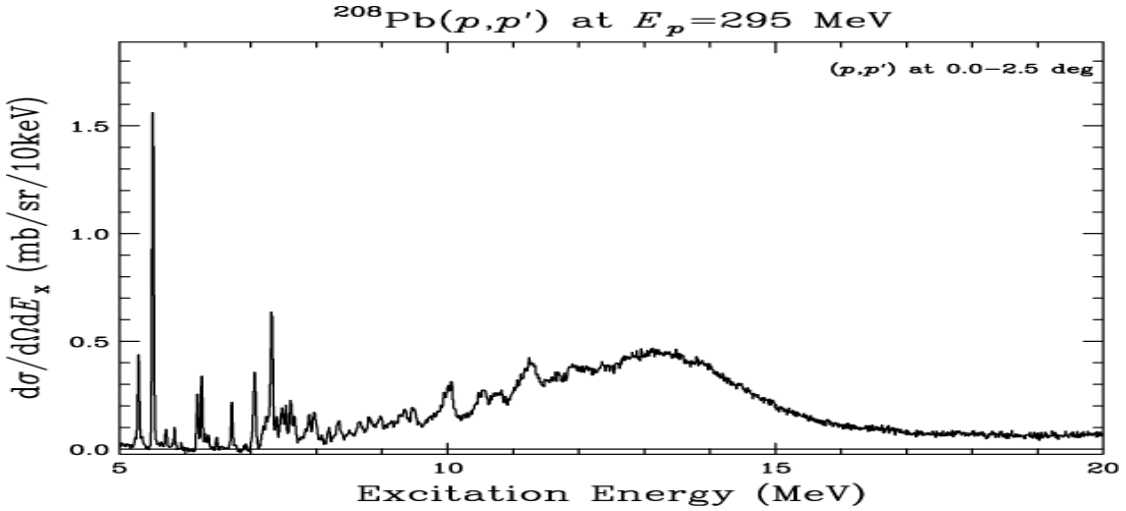

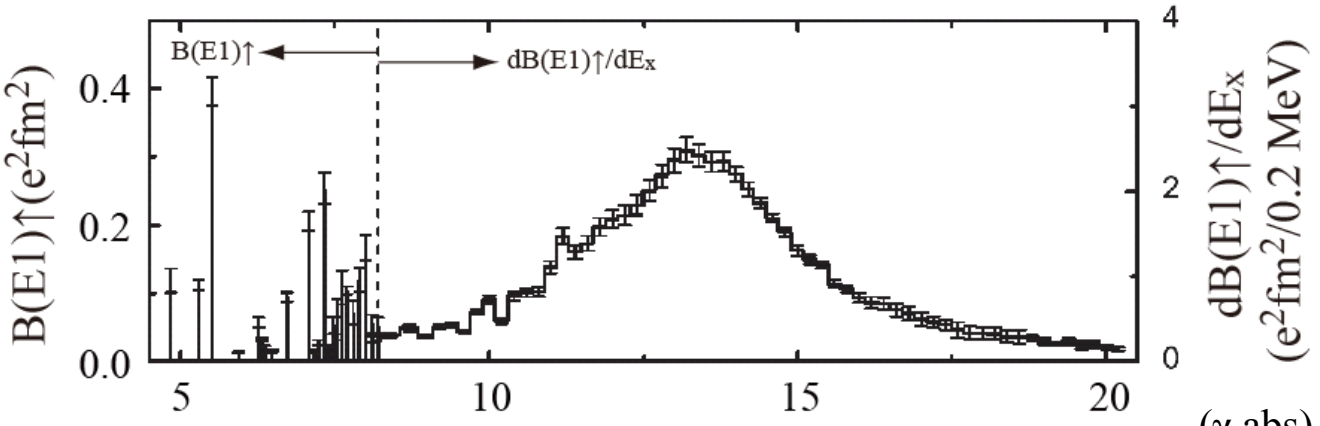

(γ,abs) at Mainz

E_x	0 – 10	10 – 20	20 – 130 MeV
α_D	2.7	16.2	1.2 fm^3

total 20.1±0.6 fm^3

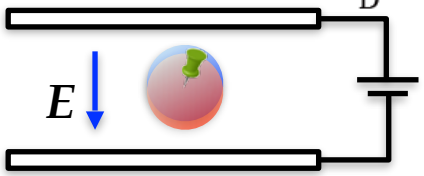

AT et al., PRL107, 062502(2011)

Electric Dipole Polarizability: ^{208}Pb, ^{120}Sn

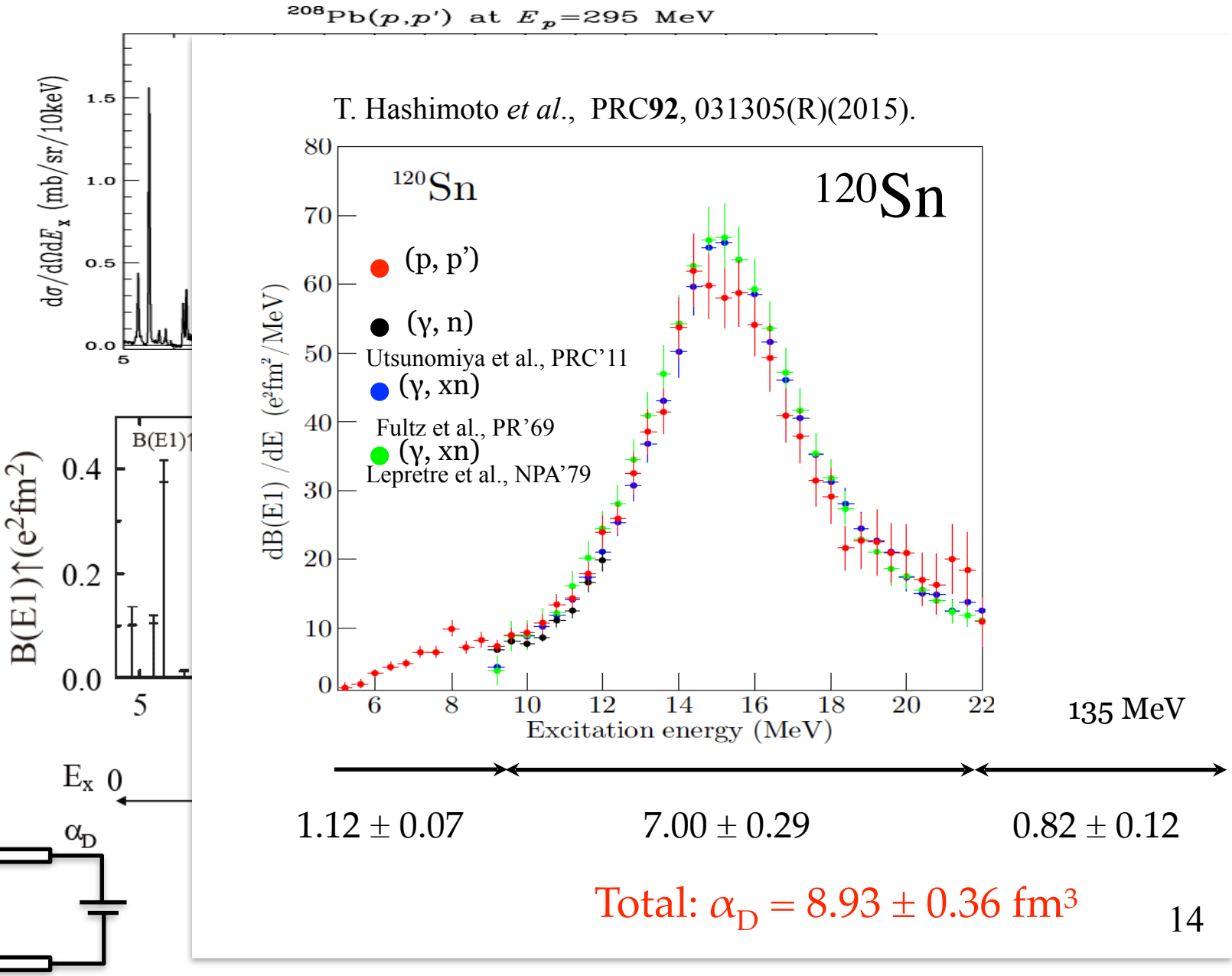

Electric Dipole Polarizability

Clear definition

Unambiguous in the integration ra

⟷ Pygmy Dipole Strength

Inversely energy weighted sum-rule

More sensitive to the low-energy st

Good convergence in the excitation

⟷ energy-weighted (TRK) s

Sum-rule for all the transitions

= Ground state property

⟷ easier comparison with th

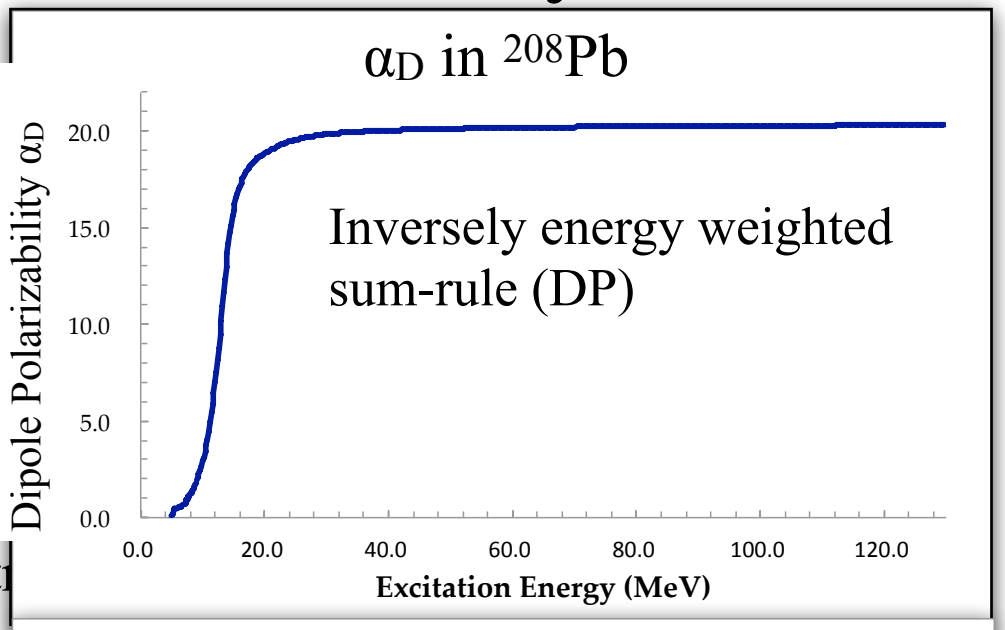

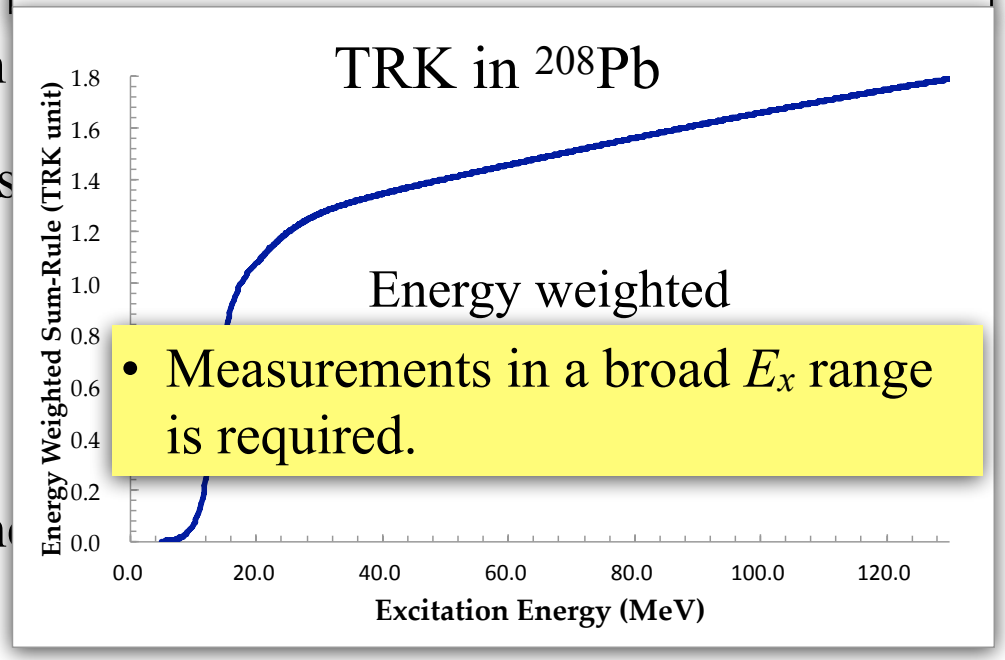

Electric Dipole Polarizability (α_D) in the correlation of J and L

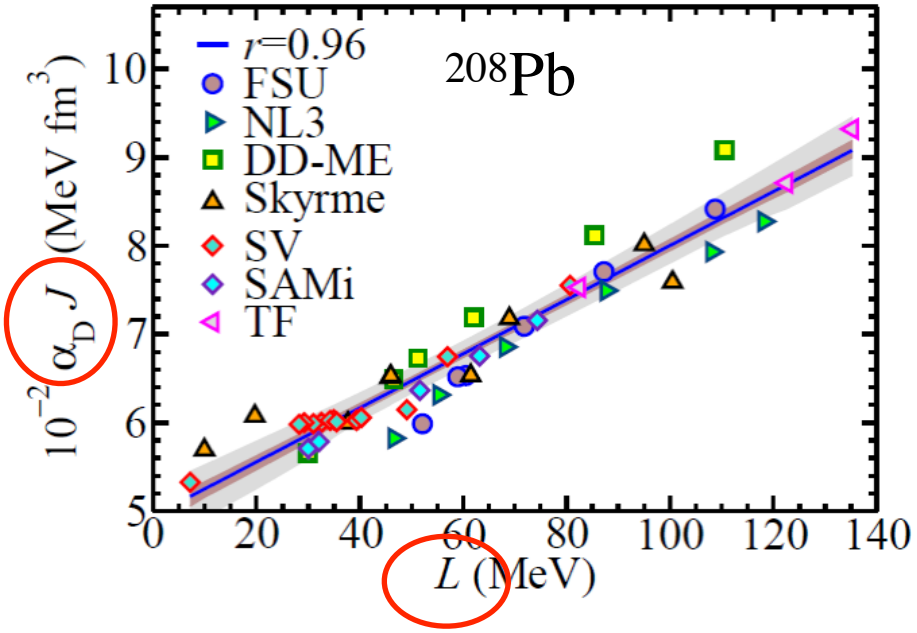

X. Roca-Maza *et al.*, PRC**88**, 024316(2013)

Correlations observed in various interaction sets in the framework of EDF.

$$\alpha_D^{\mathrm{DM}} \approx \frac{\pi e^2}{54}\frac{A\langle r^2\rangle}{J}\left[1+\frac{5}{3}\frac{L}{J}\epsilon_A\right]$$

insights from the droplet model

Precise determination of α_D of ^{208}Pb gives a constraint band in the *J*-*L* plane.

Constraints on J and L

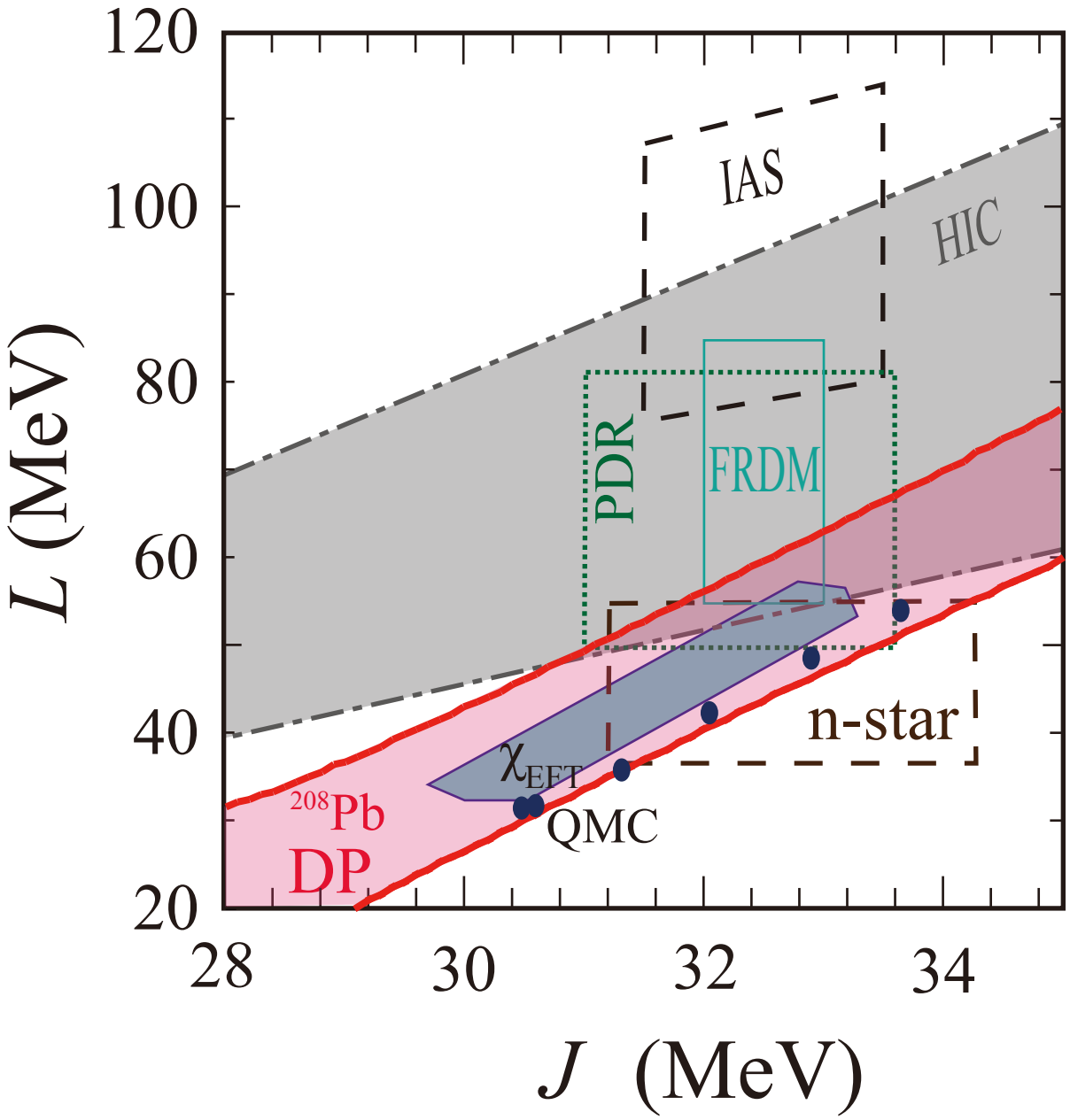

Tsang PRC2012

HIC: Heavy Ion Collision Analysis Tsang PRL2009

IAS: Isobaric Analog State Energy Danielewicz&Lee NPA2009

PDR: Pygmy Dipole Resonance in ^{132}Sn, ^{68}Ni, Carbone PRC2010

FRDM: Finite Range Droplet Model Moller PRL2012

n-star: Quiescent Low-Mass X-ray Binaries, Stainer PRL2012

χ_{EFT}: Chiral Effective Field Theory, Tews PRL2013

QMC: Quantum Monte-Carlo Calc. Gandolfi, EPJA50, 10(2014).

DP: Dipole Polarizability ^{208}Pb AT PRL2011&EPJA2014

Quasi-Deuteron Excitation Contribution

Photon absorption by a virtual deuteron in the nucleus needs to be subtracted for comparison with EDF calculations.

^{208}Pb

$\alpha_D(^{208}Pb)$: 20.1 ± 0.6 fm^3

quasi-*d*: 0.51 ± 0.15 fm^3

w/o quasi-*d*: 19.6 ± 0.6 fm^3

^{120}Sn

$\alpha_D(^{120}Sn)$: 8.93 ± 0.36 fm^3

quasi-*d*: 0.34 ± 0.08 fm^3

w/o quasi-*d*: 8.59 ± 0.37 fm^3

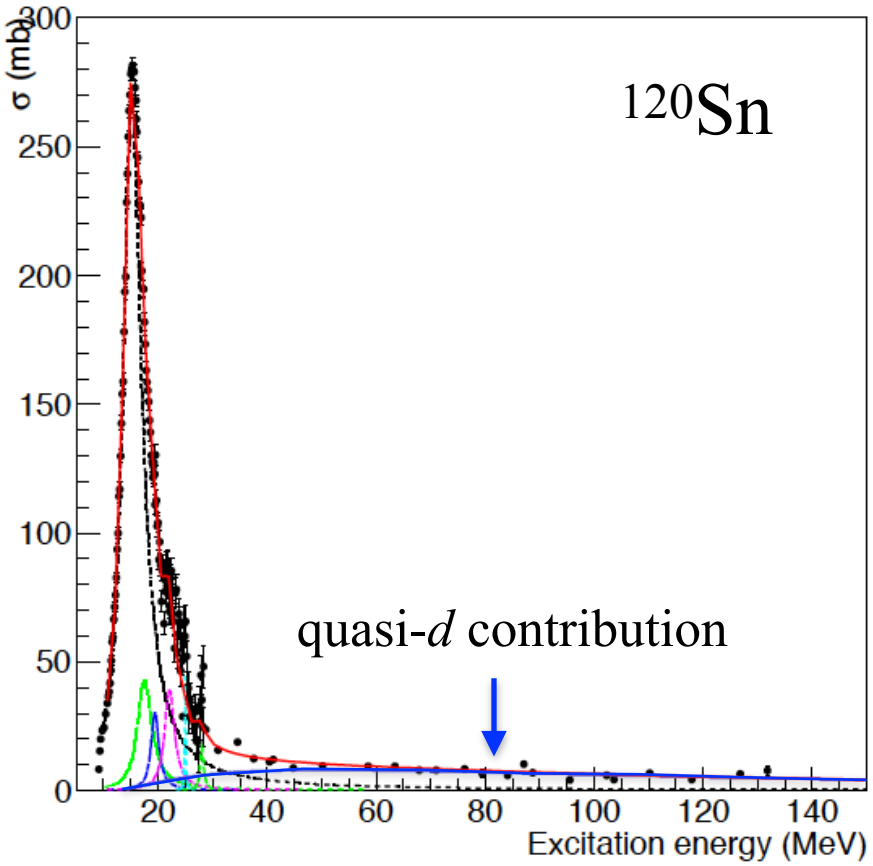

Constraints on *J*-*L* from the EDP data

X. Roca-Maza et al., PRC92, 064304(2015)

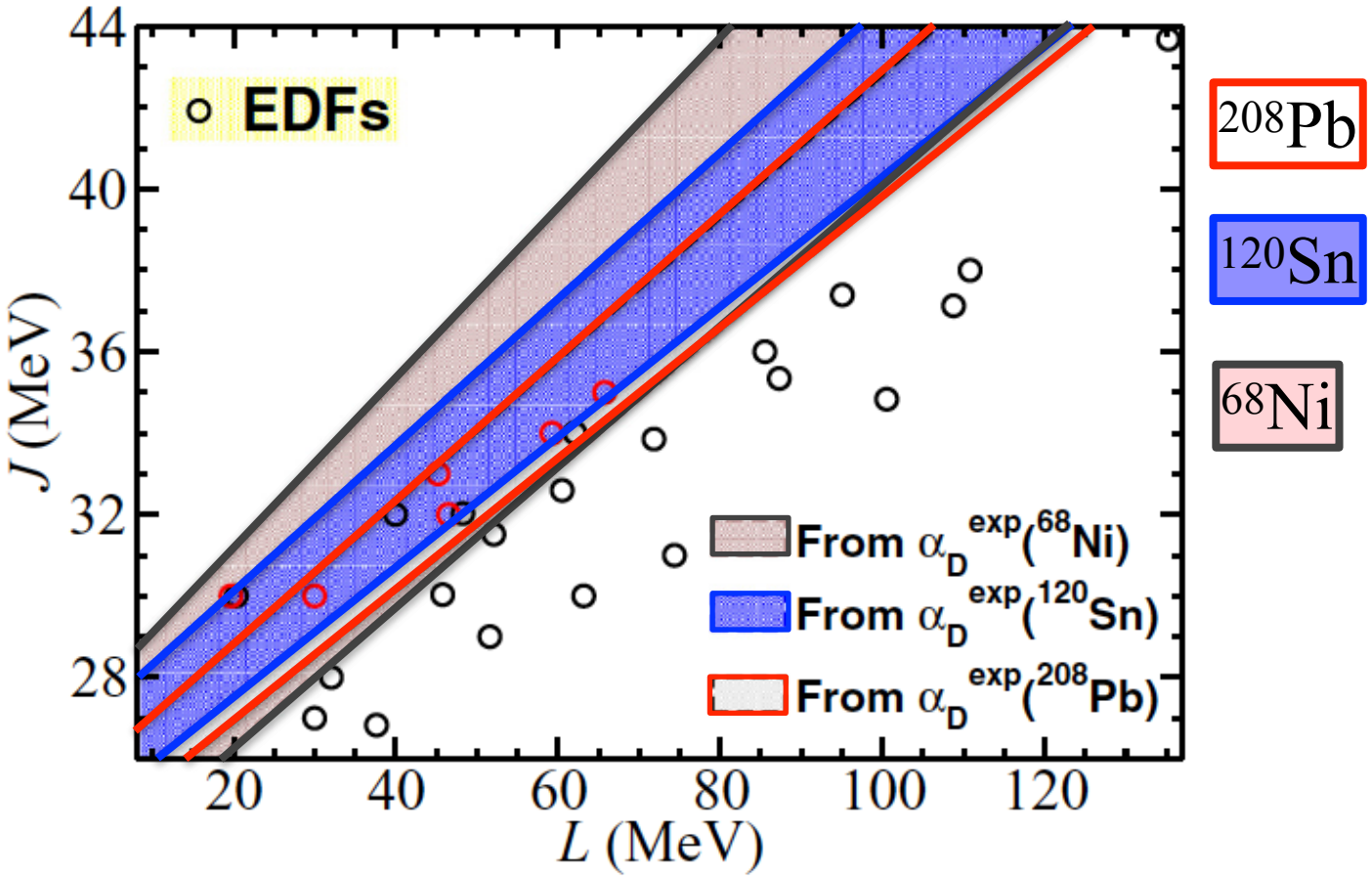

RCNP ^{208}Pb: AT *et al.*, PRL**107**, 062502 (2011).

RCNP ^{120}Sn: T. Hashimoto *et al.*, PRC**92**, 031305(R)(2015).

GSI ^{68}Ni: D.M. Rossi *et al.*, PRL**111**, 242503 (2013).

Constraints on *J*-*L* from the EDP data

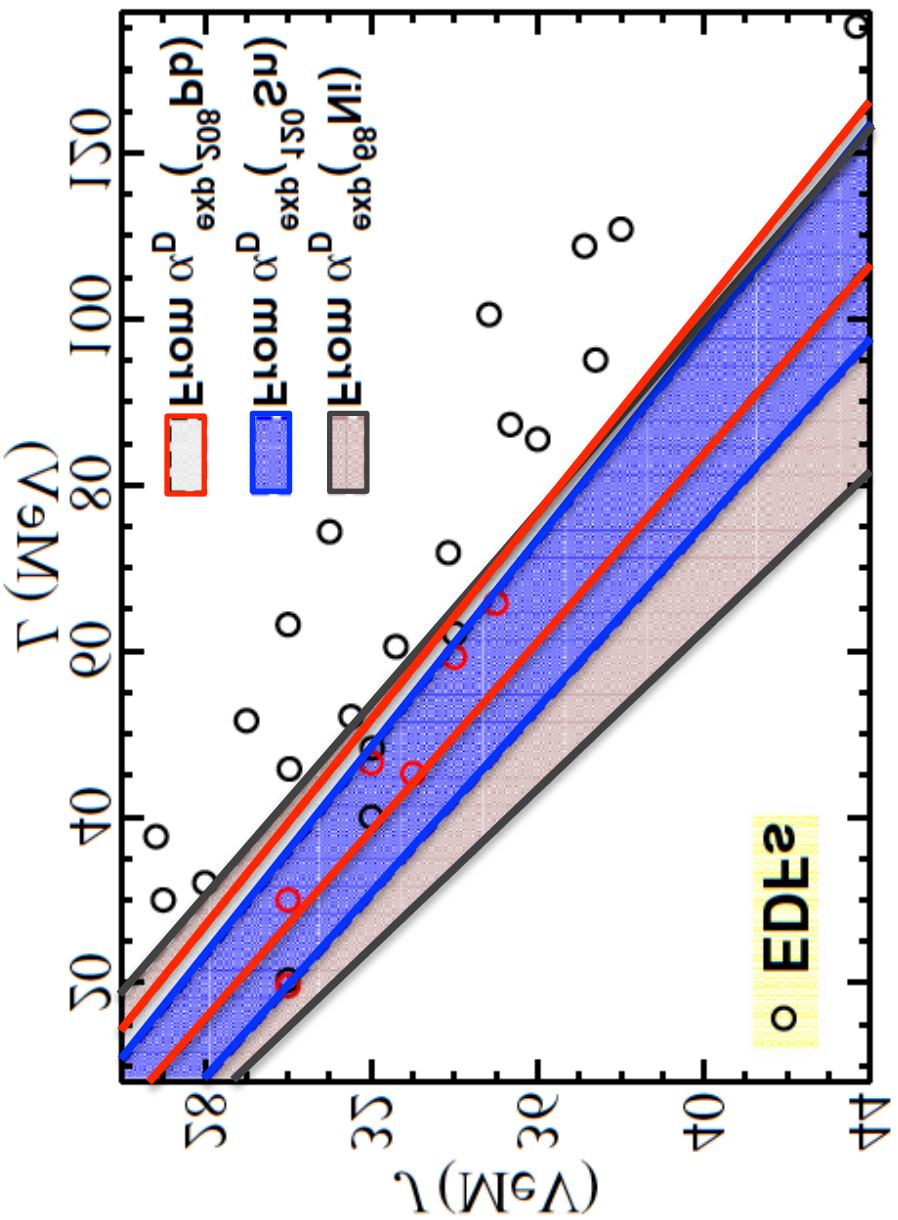

X. Roca-Maza et al., PRC92, 064304(2015)

^{208}Pb

^{120}Sn

^{68}Ni

RCNP ^{208}Pb: AT *et al.*, PRL**107**, 062502 (2011).

RCNP ^{120}Sn: T. Hashimoto *et al.*, PRC**92**, 031305(R)(2015).

GSI ^{68}Ni: D.M. Rossi *et al.*, PRL**111**, 242503 (2013).

These α_D data give essentially one constraint on the symmetry energy in the *J*-*L* plane.

Constraints on J and L

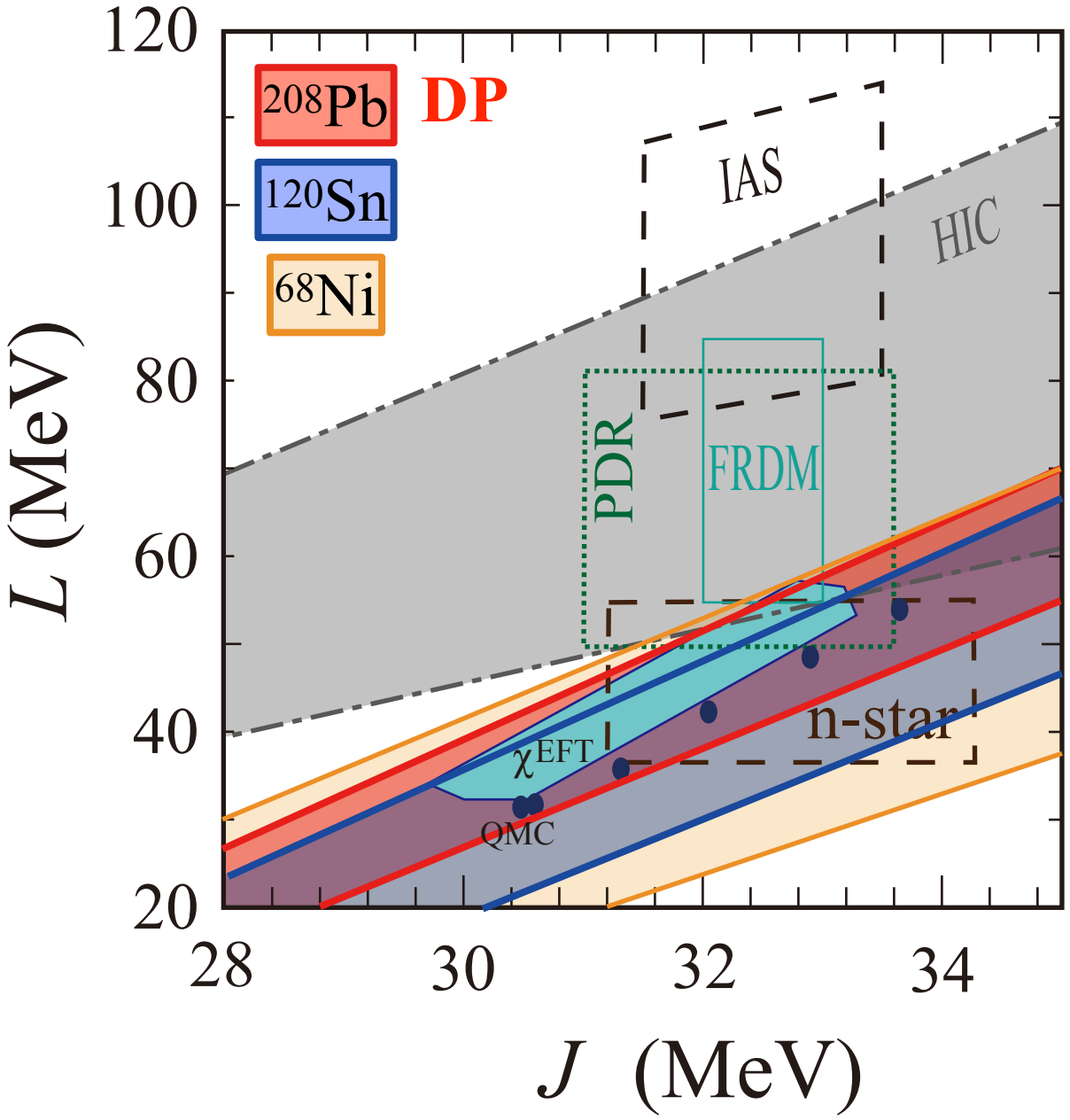

Tsang PRC2012

HIC: Heavy Ion Collision Analysis
Tsang PRL2009

IAS: Isobaric Analog State Energy
Danielewicz&Lee NPA2009

PDR: Pygmy Dipole Resonance in ^{132}Sn, ^{68}Ni, Carbone PRC2010

FRDM: Finite Range Droplet Model
Moller PRL2012

n-star: Quiescent Low-Mass X-ray Binaries, Stainer PRL2012

χ_{EFT}: Chiral Effective Field Theory, Tews PRL2013

QMC: Quantum Monte-Carlo Calc.
Gandolfi, EPJA50, 10(2014).

DP: Dipole Polarizability
^{208}Pb AT PRL2011
^{120}Sn Hashimoto PRC2015
^{68}Ni Rossi PRL2013

Constraints on J and L

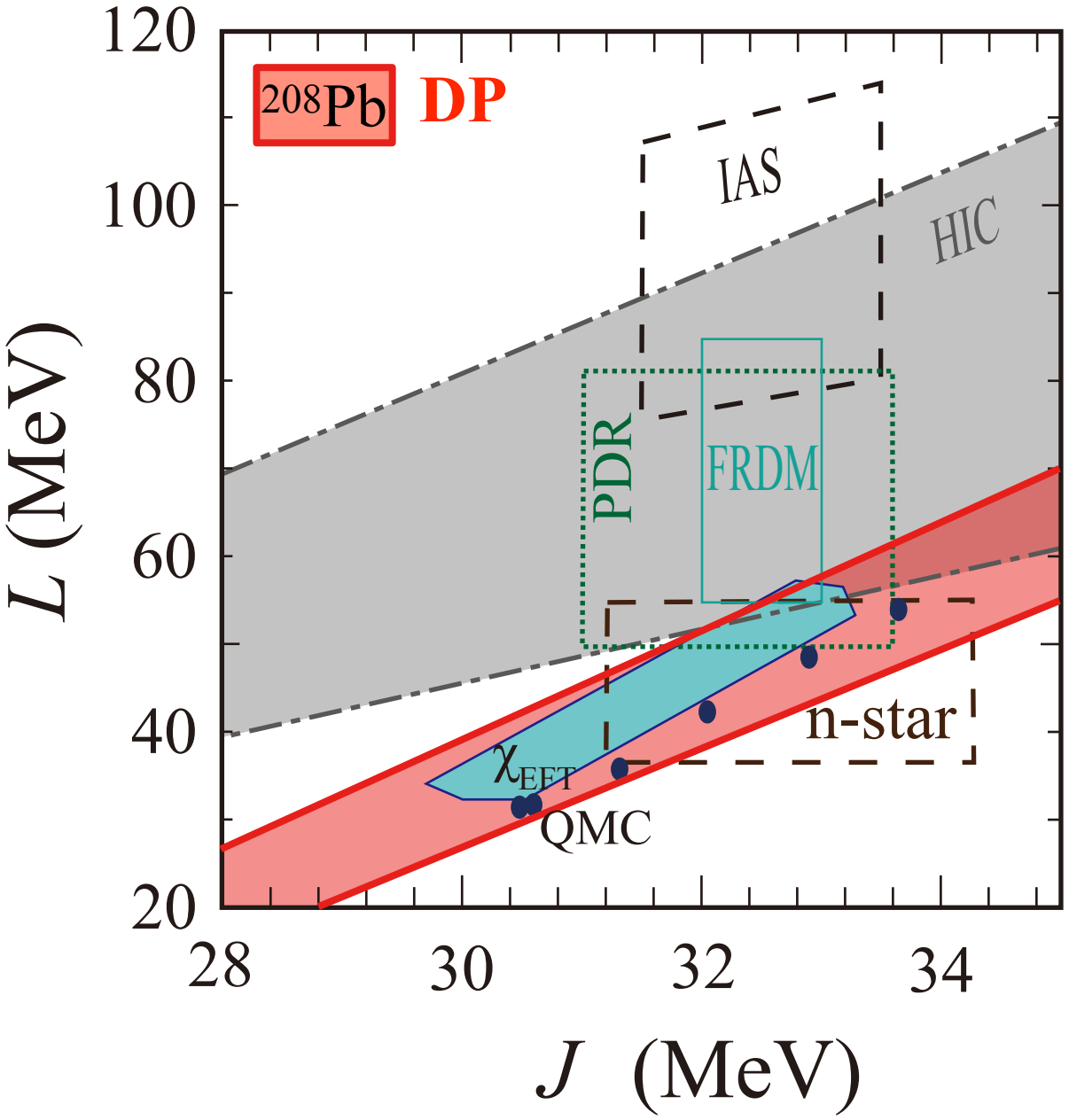

Tsang PRC2012

HIC: Heavy Ion Collision Analysis
Tsang PRL2009

IAS: Isobaric Analog State Energy
Danielewicz&Lee NPA2009

PDR: Pygmy Dipole Resonance in ^{132}Sn, ^{68}Ni, Carbone PRC2010

FRDM: Finite Range Droplet Model
Moller PRL2012

n-star: Quiescent Low-Mass X-ray Binaries, Stainer PRL2012

χ_{EFT}: Chiral Effective Field Theory, Tews PRL2013

QMC: Quantum Monte-Carlo Calc.
Gandolfi, EPJA50, 10(2014).

DP: Dipole Polarizability
^{208}Pb AT PRL2011

IAS: Isobaric Analog State Energy
Danielewicz&Lee NPA2014

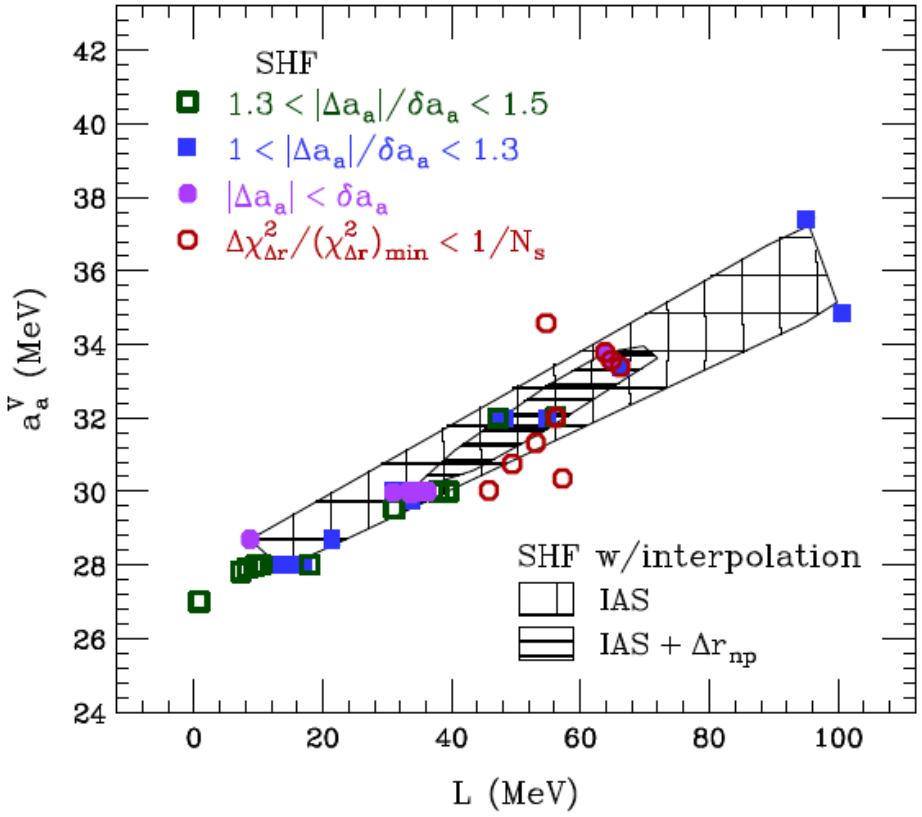

quoted neutron-skin studies

Nucleus	Reference	Data source	Δr_{np} [fm]	Δr_{np}^{GF} [fm]
^{48}Ca	Friedman [93]	pionic atoms	0.13 ± 0.06	
	Gils et al. [94]	elastic α scattering	0.175 ± 0.050	
	Ray [95]	elastic $\vec{p}$ scattering	0.229 ± 0.050	
	Clark et al. [96]	elastic p scattering	0.103 ± 0.040	
	Shlomo et al. [97]	elastic p scattering	0.10 ± 0.03	
	Gibbs et al. [98]	elastic π scattering	0.11 ± 0.04	
		combined results	0.129 ± 0.053*	0.218 ± 0.015
^{50}Ti	Gils et al. [94]	elastic α scattering	0.031 ± 0.040	0.133 ± 0.011
^{64}Ni	Ray [95]	elastic $\vec{p}$ scattering	0.167 ± 0.050	0.102 ± 0.015
^{116}Sn	Ray [95]	elastic $\vec{p}$ scattering	0.146 ± 0.050	0.103 ± 0.015
^{124}Sn	Ray [95]	elastic $\vec{p}$ scattering	0.252 ± 0.050	0.184 ± 0.021
^{204}Pb	Zenihiro et al. [99]	elastic p scattering	0.178 ± 0.059	0.161 ± 0.024
^{206}Pb	Zenihiro et al. [99]	elastic p scattering	0.180 ± 0.064	
	Starodubsky et al. [100]	elastic p scattering	0.181 ± 0.045	
		combined results	0.181 ± 0.037	0.172 ± 0.024
^{207}Pb	Starodubsky et al. [100]	elastic p scattering	0.186 ± 0.041	0.178 ± 0.024
^{208}Pb	Starodubsky et al. [100]	elastic p scattering	0.197 ± 0.042	
	Ray [95]	elastic $\vec{p}$ scattering	0.16 ± 0.05	
	Clark et al. [96]	elastic p scattering	0.119 ± 0.045	
	Zenihiro et al. [99]	elastic p scattering	0.211 ± 0.063	
	Friedman [93]	elastic π^+ scattering	0.11 ± 0.06	
	Friedman [93]	pionic atoms	0.15 ± 0.08	
		combined results	0.159 ± 0.041*	0.179 ± 0.023

any average effects of asymmetry on the reactions competing with a variety of physical effects subject to modeling uncertainties. In this paper we attempt to learn about the average effects of neutron–proton asymmetry on nuclear energies, exploiting excitation energies to isobaric analog states and to reach the conclusions in as model-independent manner as possible. Our early efforts in this direction have been reported in [1–3]. As we progress, we find that we need to reassess our strategy.

Determination of Neutron Density Distribution by Strong Interaction

Polarized proton elastic scattering at 295 MeV (RCNP, Osaka University)
Analysis with relativistic impulse approximation (RIA), medium modification fixed with ^{58}Ni data

ds/dW, Ay

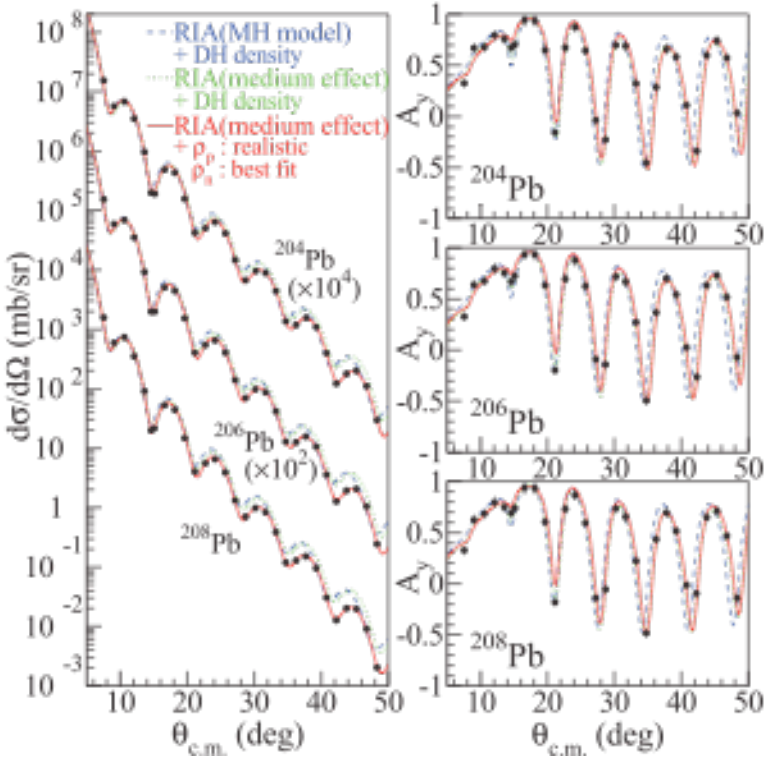

RIA + Medium Effect

$r_n(r)$

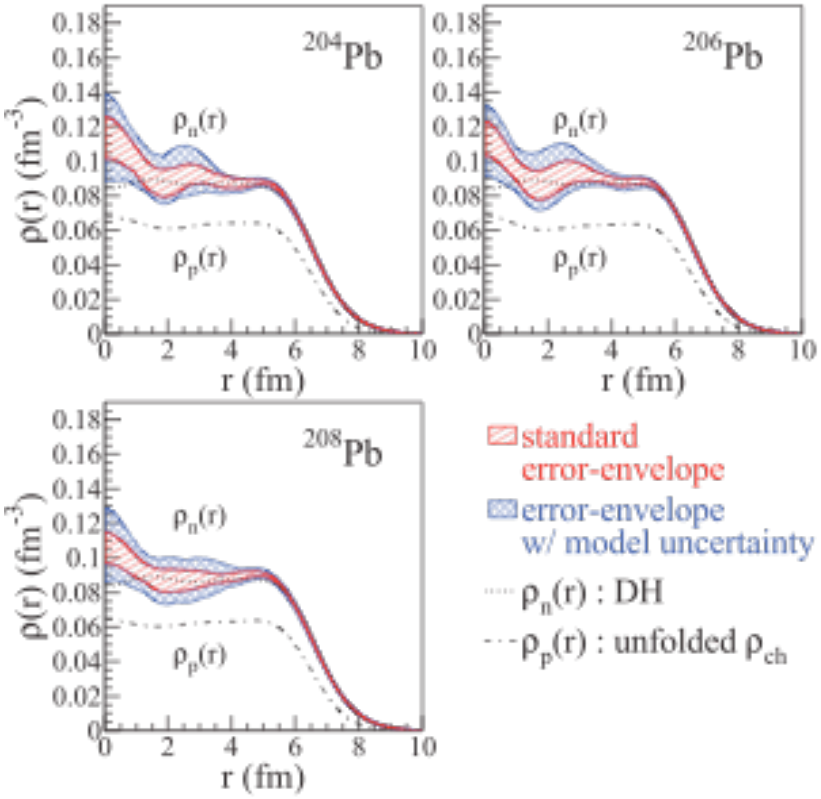

$\Delta r_n/r_n < 0.5\%$

J.Zenihiro et al., PRC 82, 044611 (2010)

Constraints on J and L

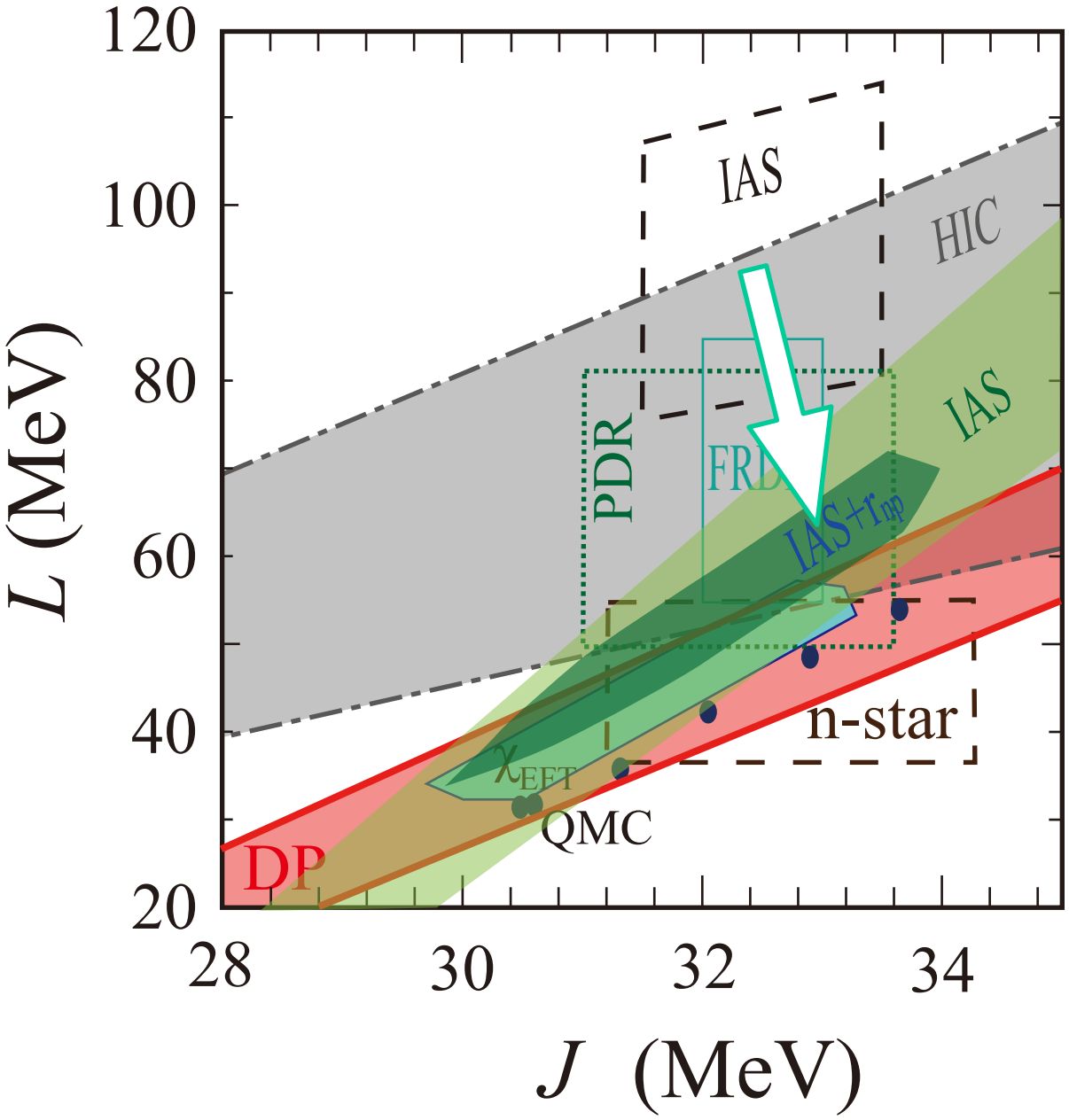

Tsang PRC2012

HIC: Heavy Ion Collision Analysis
Tsang PRL2009

IAS: Isobaric Analog State Energy
Danielewicz&Lee **NPA2009→2014**

PDR: Pygmy Dipole Resonance in
^{132}Sn, ^{68}Ni, Carbone PRC2010

FRDM: Finite Range Droplet Model
Moller PRL2012

n-star: Quiescent Low-Mass X-ray Binaries, Stainer PRL2012

χ_{EFT}: Chiral Effective Field Theory, Tews PRL2013

QMC: Quantum Monte-Carlo Calc.
Gandolfi, EPJA50, 10(2014).

DP: Dipole Polarizability
^{208}Pb AT PRL2011

Constraints on J and L

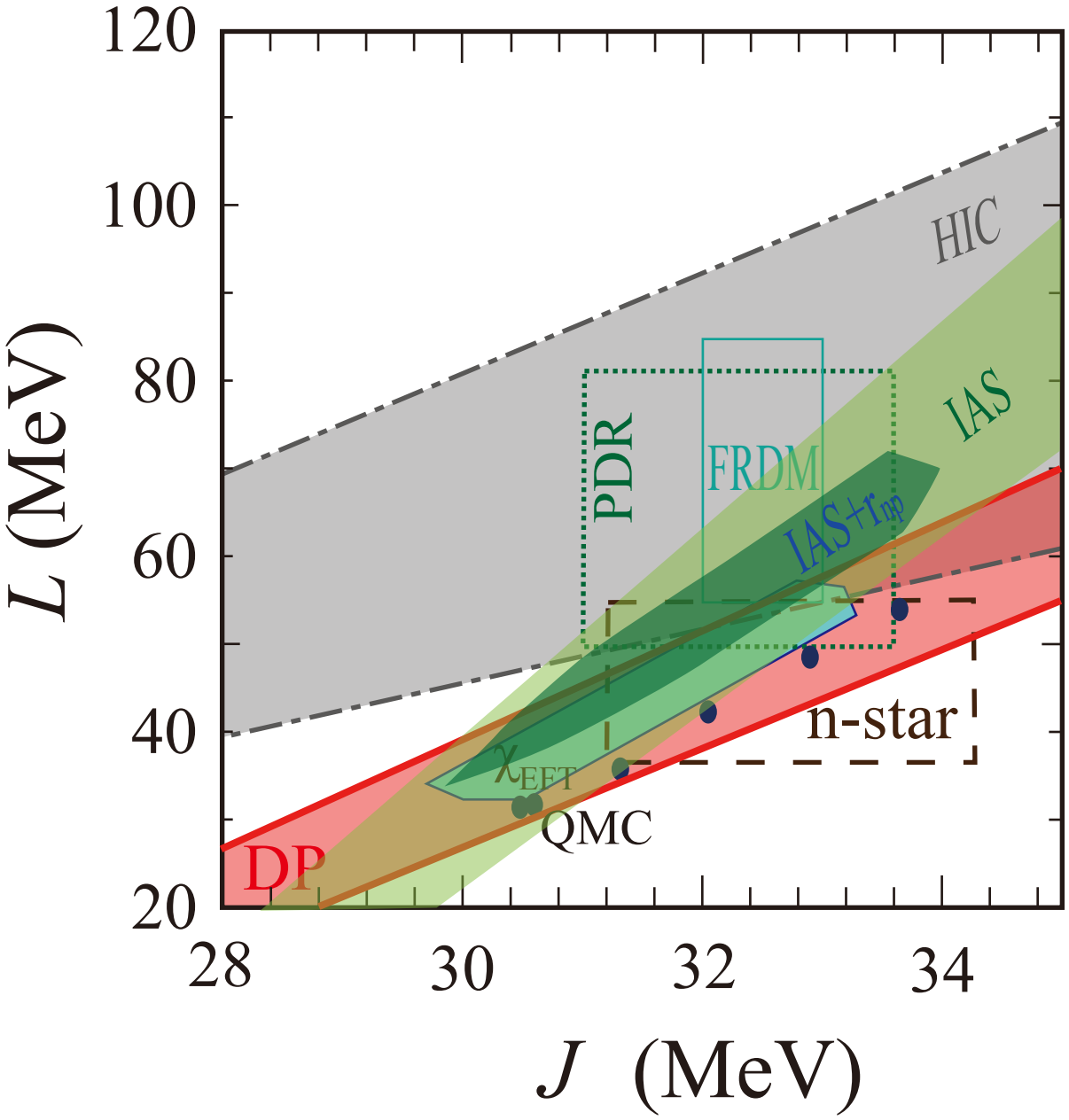

Tsang PRC2012

HIC: Heavy Ion Collision Analysis Tsang PRL2009

IAS: Isobaric Analog State Energy Danielewicz&Lee NPA2014

PDR: Pygmy Dipole Resonance in ^{132}Sn, ^{68}Ni, Carbone PRC2010

FRDM: Finite Range Droplet Model Moller PRL2012

n-star: Quiescent Low-Mass X-ray Binaries, Stainer PRL2012

χ_{EFT}: Chiral Effective Field Theory, Tews PRL2013

QMC: Quantum Monte-Carlo Calc. Gandolfi, EPJA50, 10(2014).

DP: Dipole Polarizability ^{208}Pb AT PRL2011

LA-UR-16-26401 Sagawa and Moller

The optimal values of the asymmetry variables J and L that we obtained from the mass model FRDM (2012) study are

$$J = 32.3 \pm 0.5 \text{ MeV}$$
$$L = 53.5 \pm 15 \text{ MeV}$$

with the minimum rms deviation of σ <560 keV as shown in Fig. 2. The above optimal L value is somewhat smaller than the value in Ref. [3], because we have implemented a more accurate calculation of the zero-point fluctuation effect, see [2] for more details.

FRDM: Finite Range Droplet Model
Moeller ADNTD2016

Constraints on J and L

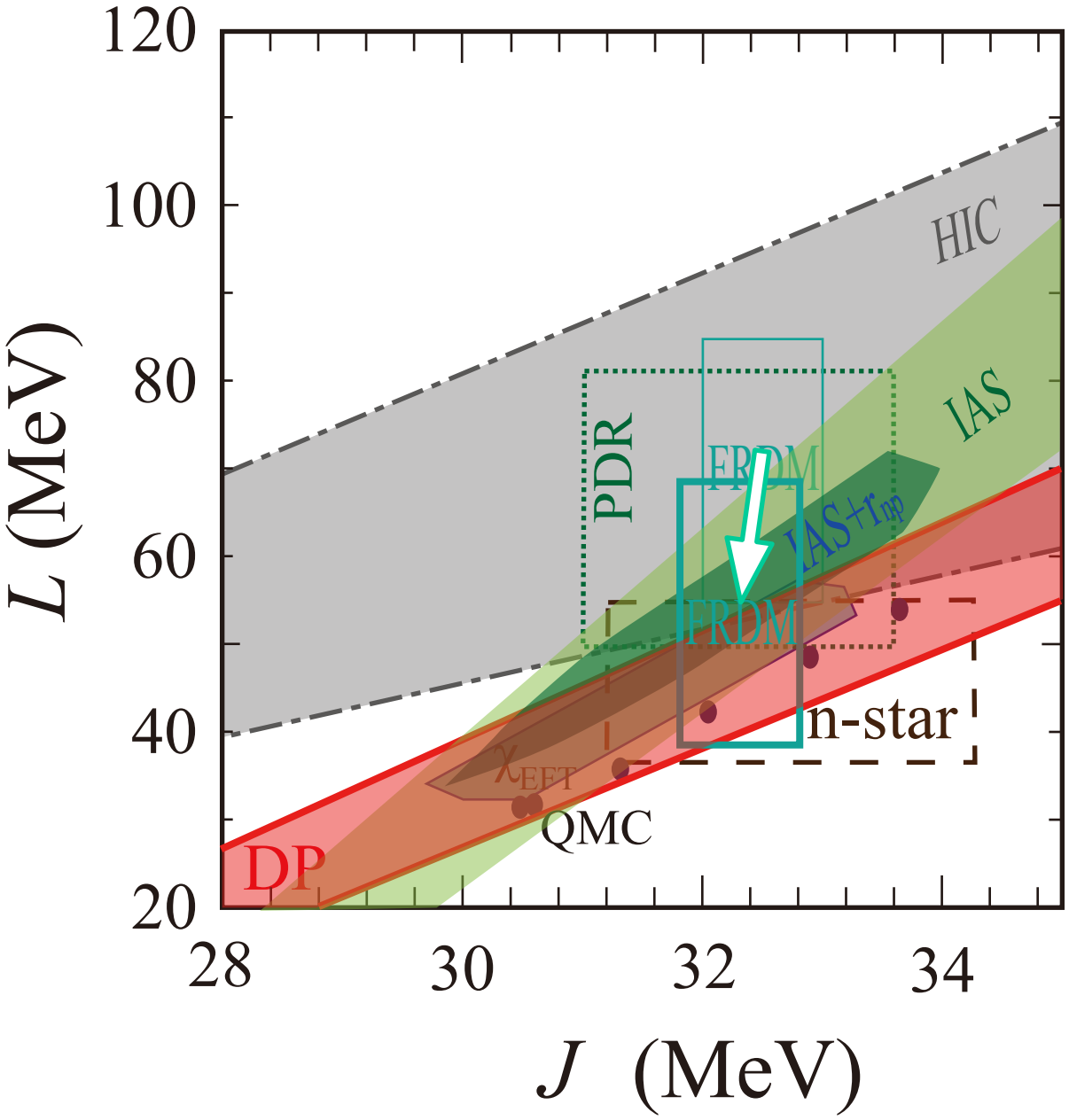

Tsang PRC2012

HIC: Heavy Ion Collision Analysis
Tsang PRL2009

IAS: Isobaric Analog State Energy
Danielewicz&Lee NPA2014

PDR: Pygmy Dipole Resonance in ^{132}Sn, ^{68}Ni, Carbone PRC2010

FRDM: Finite Range Droplet Model
Moller **PRL2012→ADNTD2016**

n-star: Quiescent Low-Mass X-ray Binaries, Stainer PRL2012

χ_{EFT}: Chiral Effective Field Theory, Tews PRL2013

QMC: Quantum Monte-Carlo Calc.
Gandolfi, EPJA50, 10(2014).

DP: Dipole Polarizability
^{208}Pb AT PRL2011

Constraints on J and L

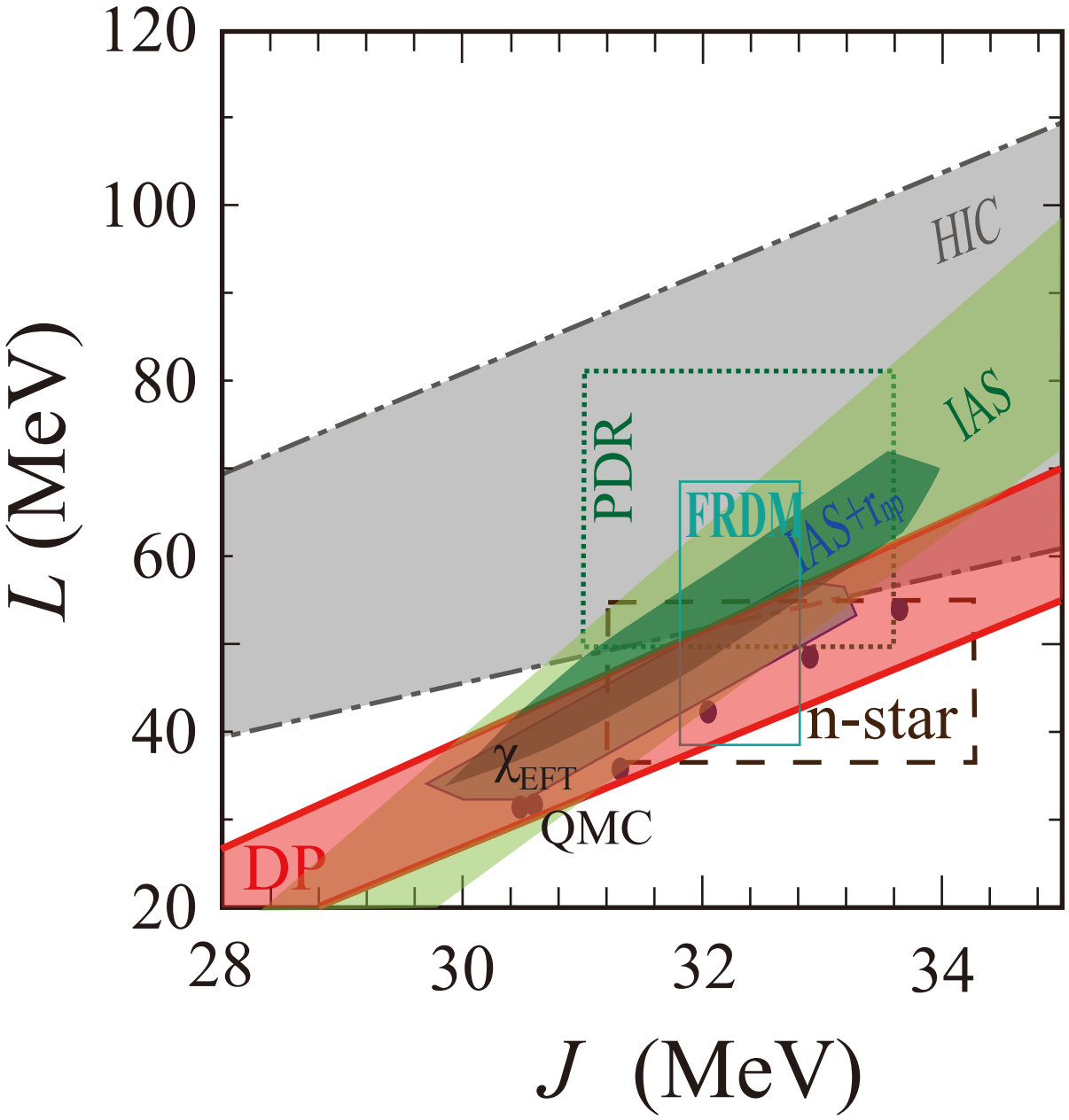

Tsang PRC2012

HIC: Heavy Ion Collision Analysis
Tsang PRL2009

IAS: Isobaric Analog State Energy
Danielewicz&Lee NPA2014

PDR: Pygmy Dipole Resonance in ^{132}Sn, ^{68}Ni, Carbone PRC2010

FRDM: Finite Range Droplet Model
Moller ADNTD2016

n-star: Quiescent Low-Mass X-ray Binaries, Stainer PRL2012

χ_{EFT}: Chiral Effective Field Theory, Tews PRL2013

QMC: Quantum Monte-Carlo Calc.
Gandolfi, EPJA50, 10(2014).

DP: Dipole Polarizability
^{208}Pb AT PRL2011

PDR: Pygmy Dipole Resonance in ^{132}Sn, ^{68}Ni, Carbone PRC2010

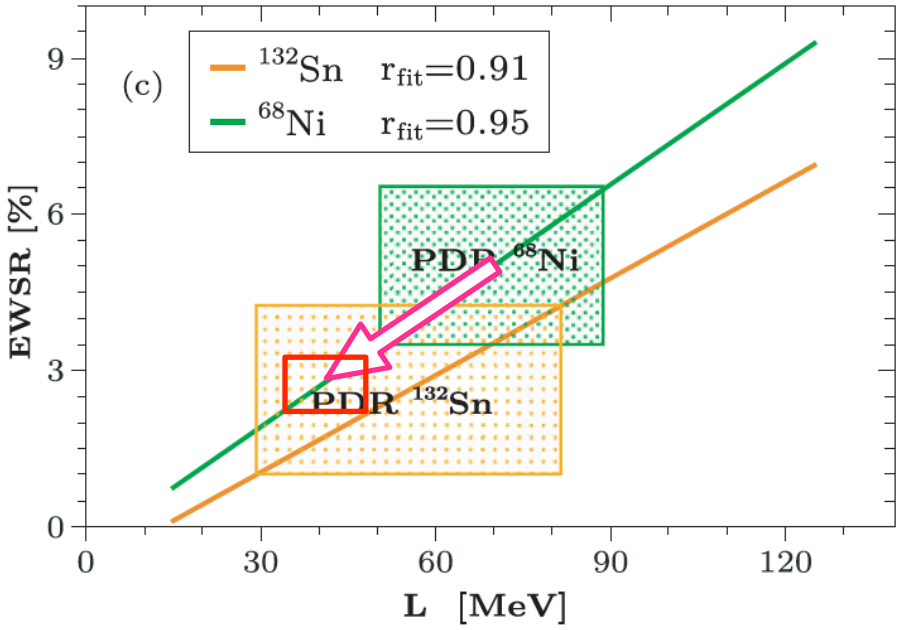

Wieland: PRL2009

In summary, we have here presented the first experimental search of a pygmy resonance in the neutron-rich ^{68}Ni nucleus using the virtual photon scattering technique. Evidence is found for the presence of sizeable strength energetically located below the GDR and centered at ≈11 MeV with approximately 5% of the EWSR strength.

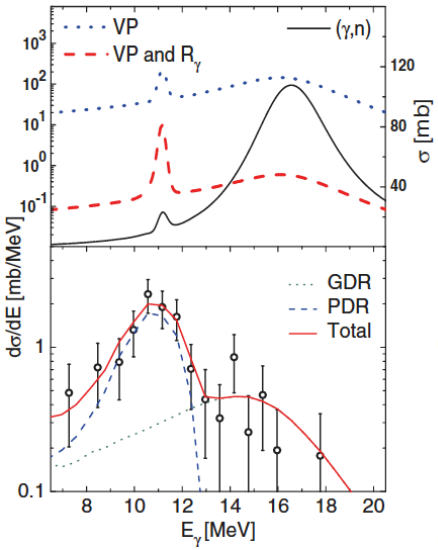

Rossi: PRL2013

TABLE I. GDR and PDR parameters for ^{68}Ni from fit to $E1$ strength, as shown in Fig. 3. Included as well are the GDR and PDR parameters from the literature.

			This work	Literature	Reference
GDR	E_m	[MeV]	17.1(2)	17.84	[30]
	Γ	[MeV]	6.1(5)	5.69	[30]
	S_{EWSR}	[%]	98(7)	100	
PDR	E_m	[MeV]	9.55(17)	11.0(5)	[25,31]
	σ	[MeV]	0.51(13)	<1	[25]
	S_{EWSR}	[%]	2.8(5)	5.0(1.5)	[13,25]

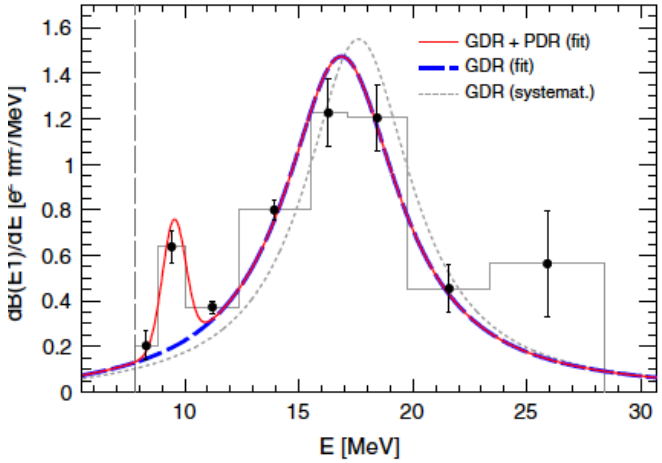

Constraints on J and L

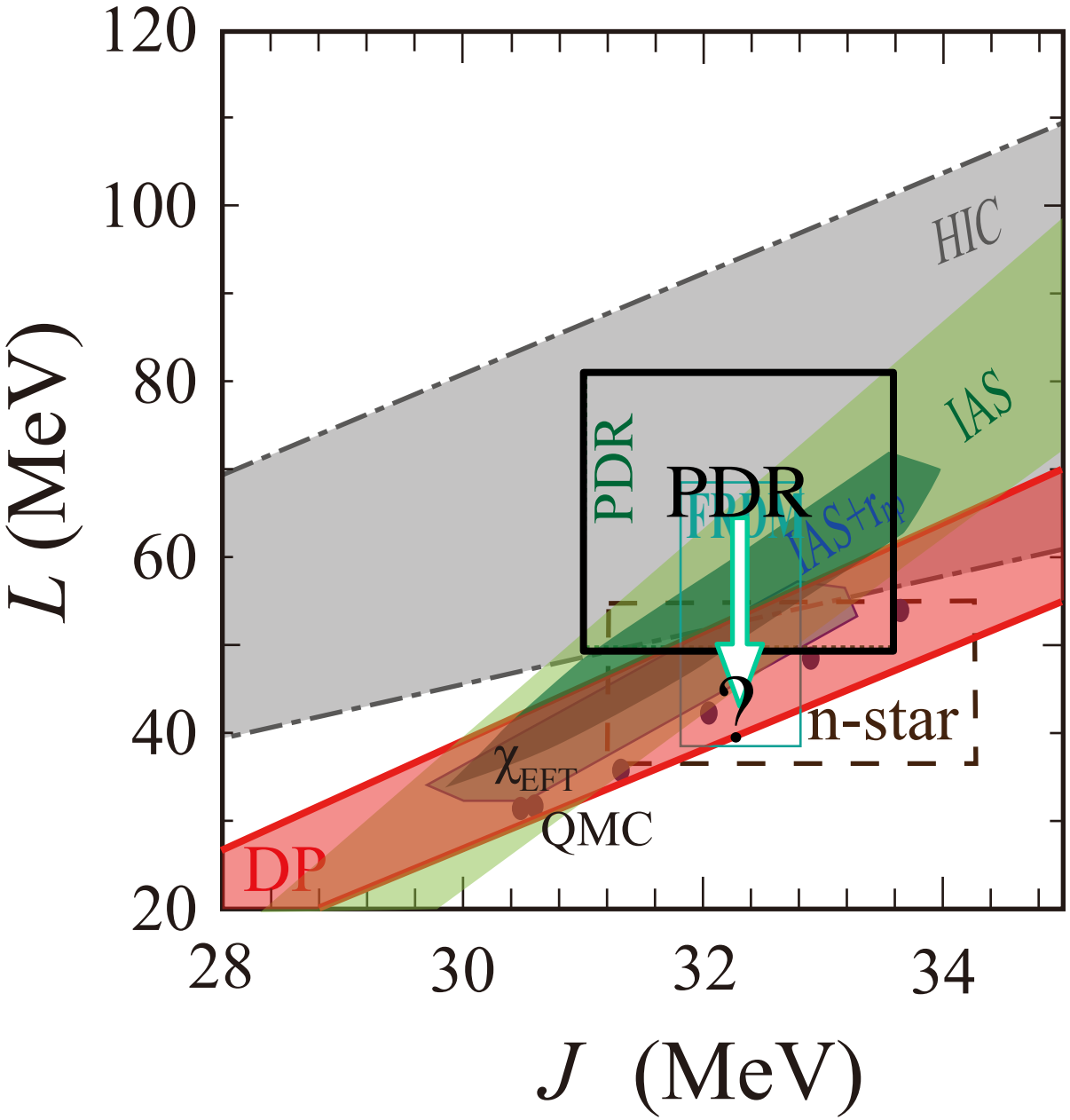

Tsang PRC2012

HIC: Heavy Ion Collision Analysis
Tsang PRL2009

IAS: Isobaric Analog State Energy
Danielewicz&Lee NPA2014

PDR: Pygmy Dipole Resonance in ^{132}Sn, ^{68}Ni, Carbone **PRC2010→?**

FRDM: Finite Range Droplet Model
Moller ADNTD2016

n-star: Quiescent Low-Mass X-ray Binaries, Stainer PRL2012

χ_{EFT}: Chiral Effective Field Theory, Tews PRL2013

QMC: Quantum Monte-Carlo Calc.
Gandolfi, EPJA50, 10(2014).

DP: Dipole Polarizability
^{208}Pb AT PRL2011

Dipole Polarizability of ^{48}Ca

where the EDF and ab-initio calculations meet

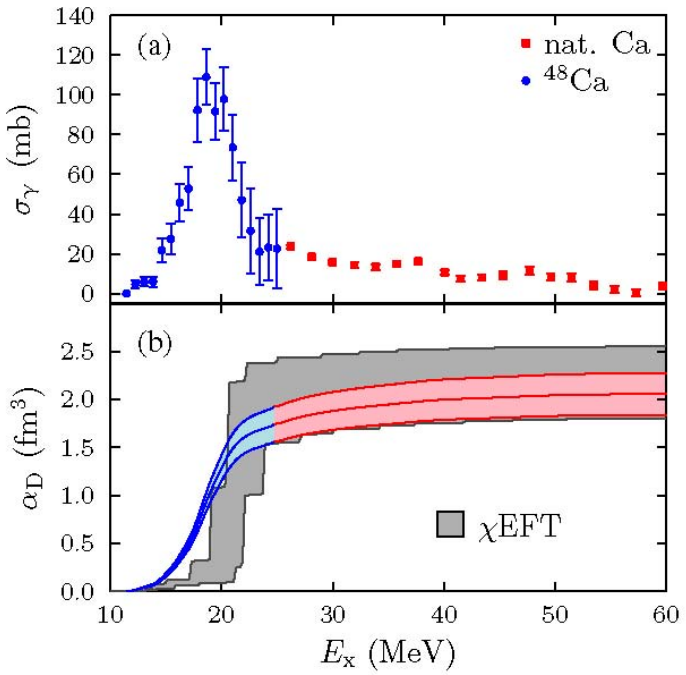

J. Birkhan et al., PRL118_252501(2017)

Theory: Darmstadt-Tennessee-TRIUMF

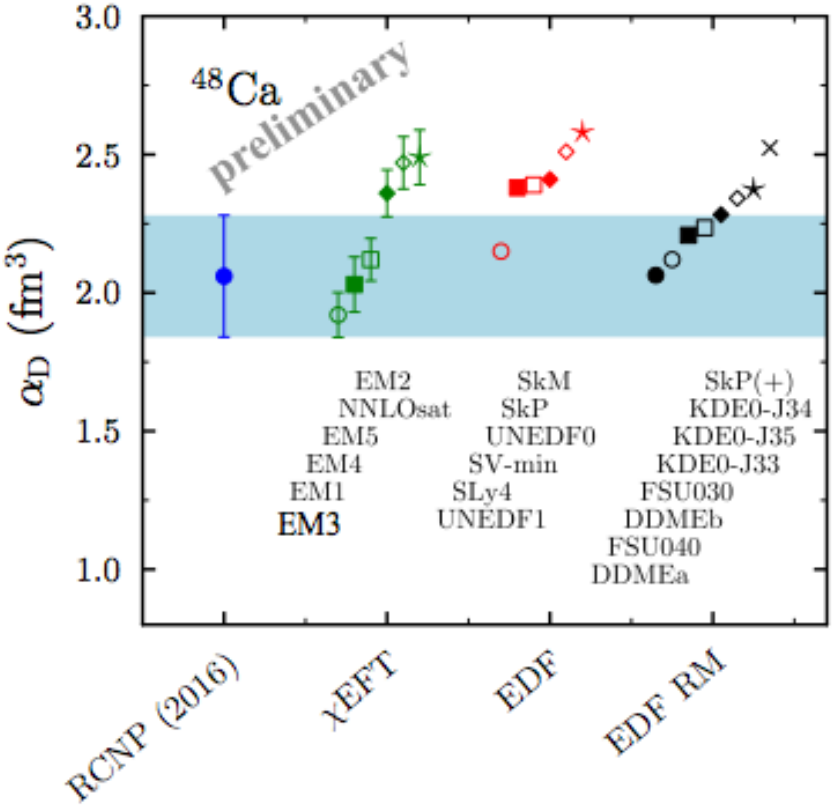

A dedicated new measurement is approved for a smaller uncertainty.

QMC

S. Gandolfi, J. Carlson et al., EPJA50, 10 (2014)

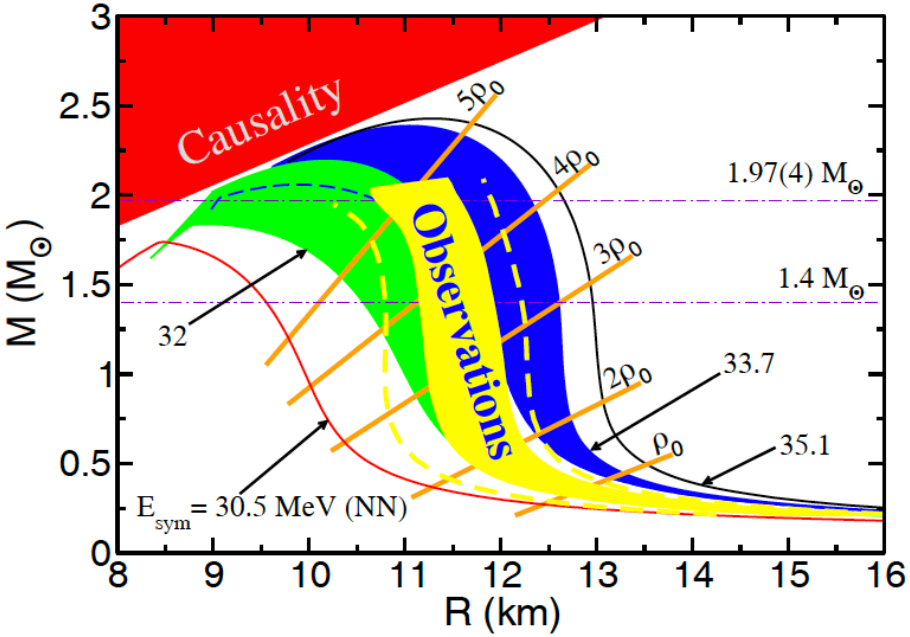

χEFT

I. Tews, K. Hebeler et al., PRL110, 032504(2013)

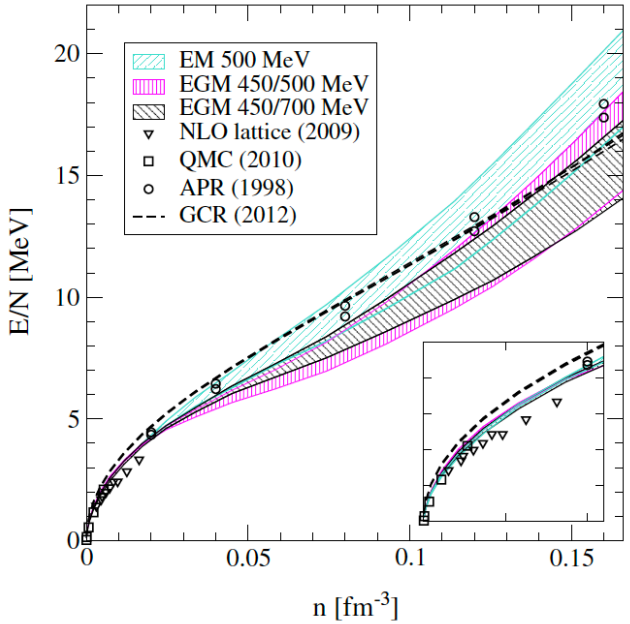

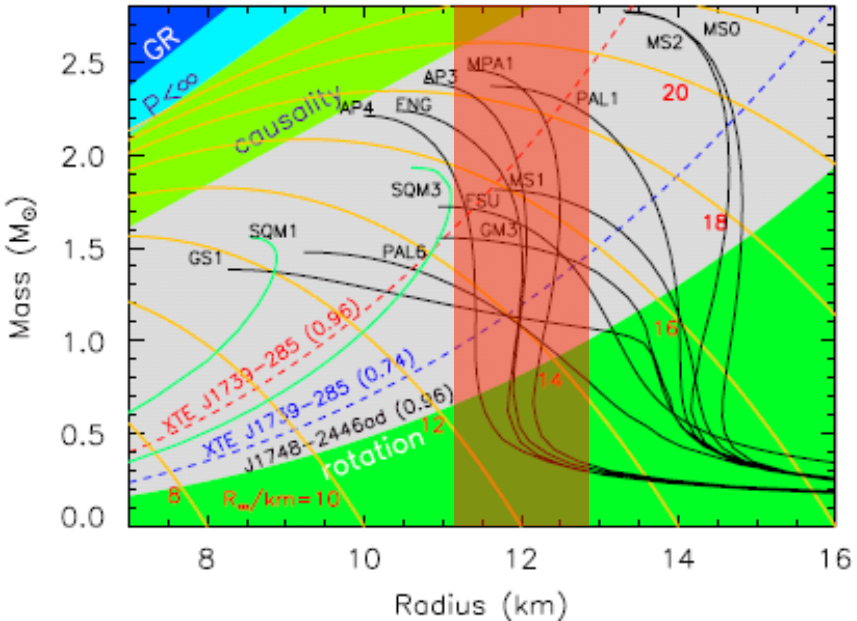

Neutron Star Merger GW

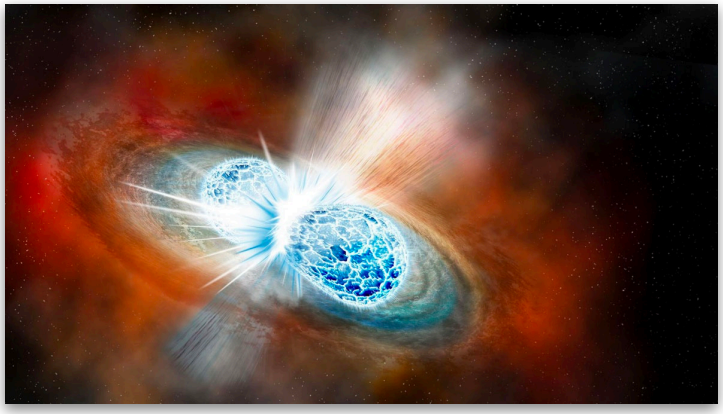

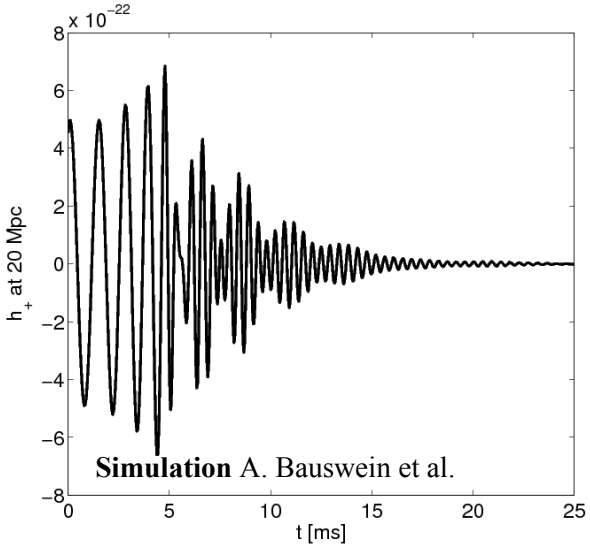

GW
PRL119, 161101(2017)

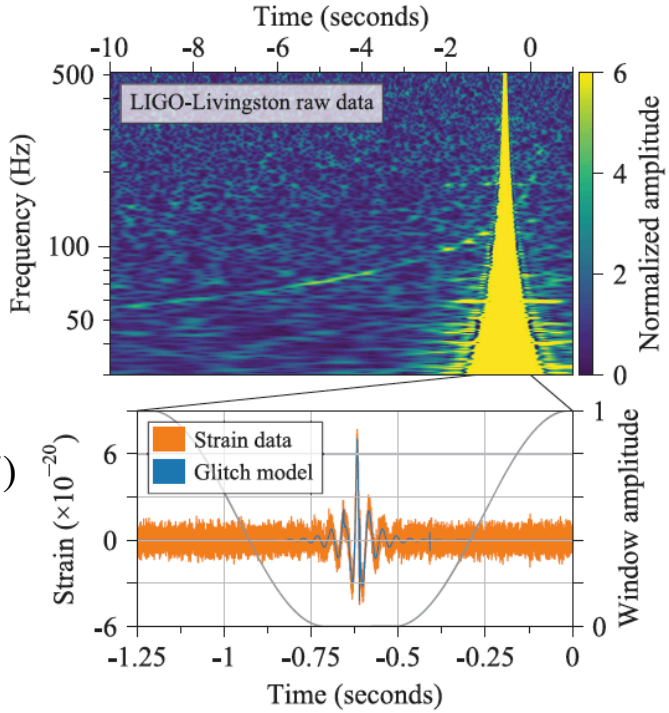

Advanced LIGO

Neutron Star Merger GW

PRL119, 161101(2017)

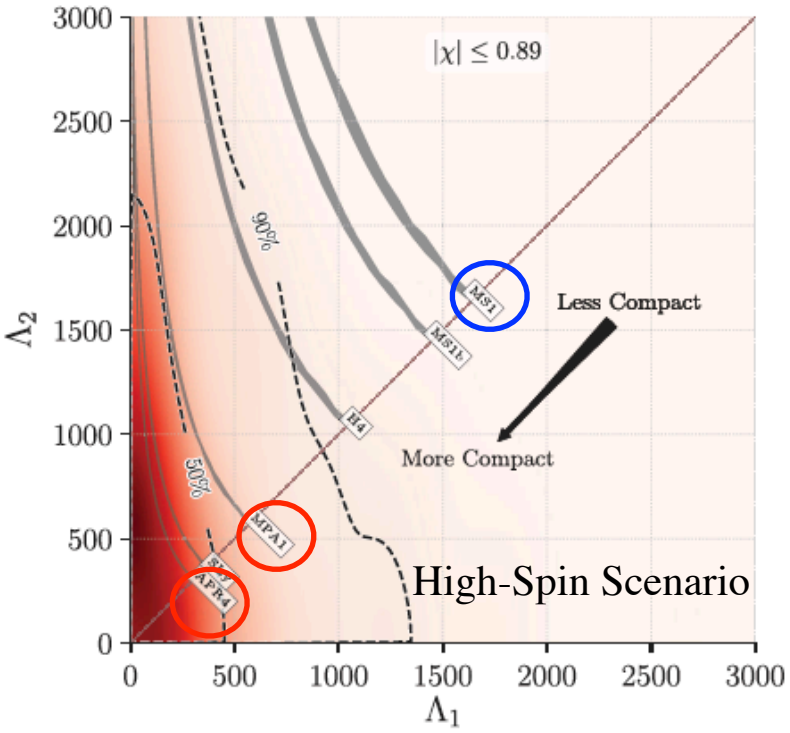

High-Spin Scenario

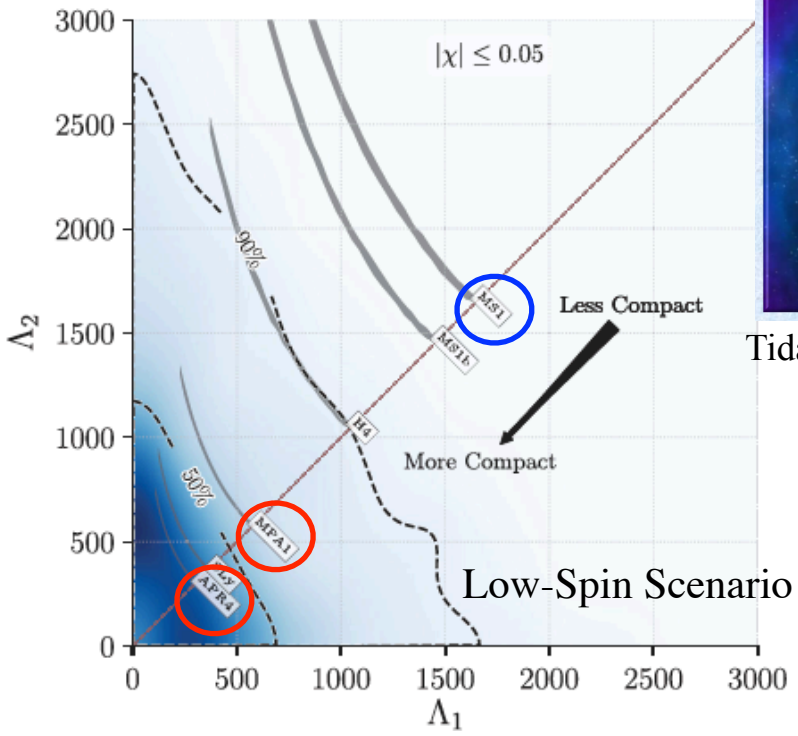

Low-Spin Scenario

Tidal Deformatio

Tidal Deformation Parameters

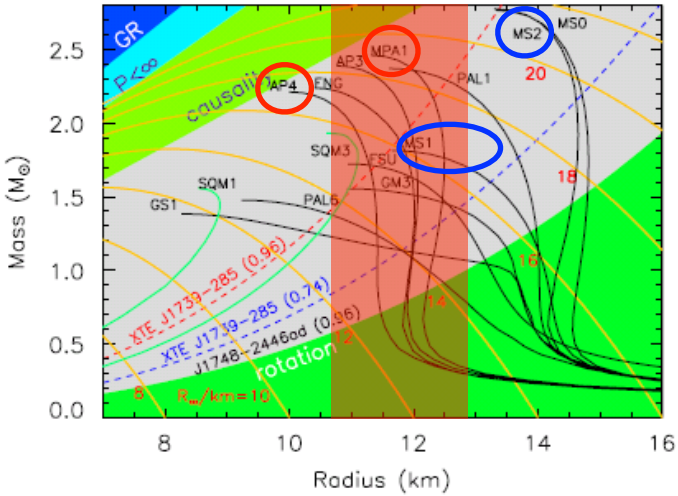

Giant Monopole Resonances and the Nuclear Incompressibility

For the equation of state of symmetric nuclear matter at saturation nuclear density:

$$\left[\frac{d(E/A)}{d\rho}\right]_{\rho=\rho_0} = 0$$

and one can derive the incompressibility of nuclear matter:

$$K_{nm} = \left[9\rho^2 \frac{d^2(E/A)}{d\rho^2}\right]_{\rho=\rho_0}$$

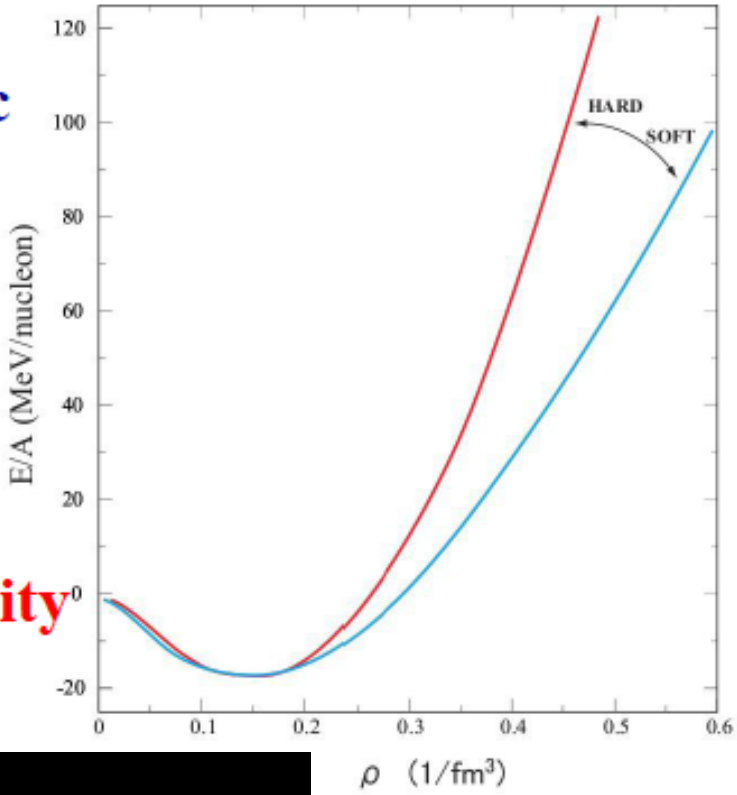

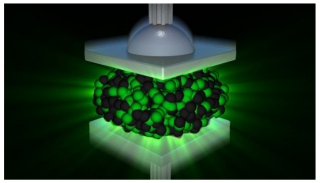

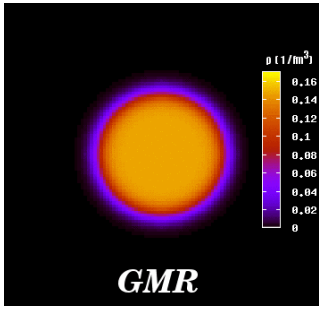

by M. Itoh

***E/A*: binding energy per nucleon**

ρ : nuclear density

ρ_0 : nuclear density at saturation

J.P. Blaizot, Phys. Rep. 64 (1980) 171

Courtesy of M.N. Harakeh

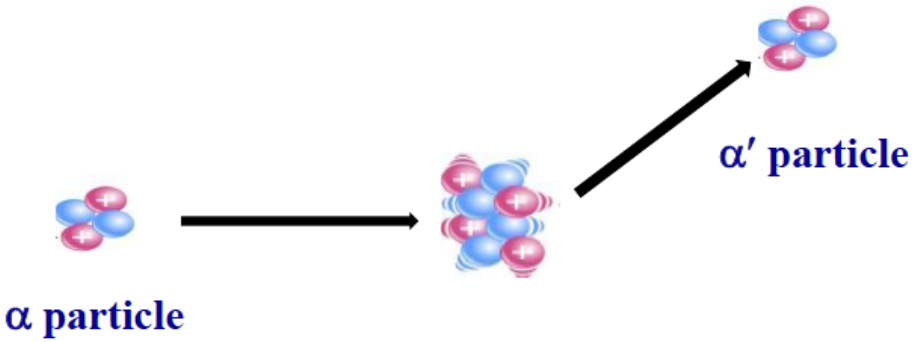

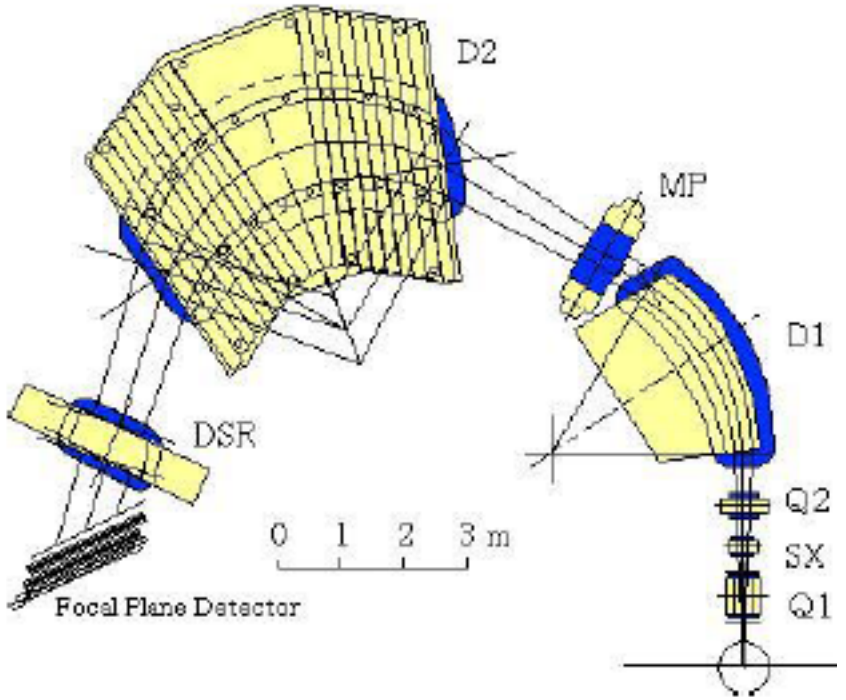

Grand Raiden@

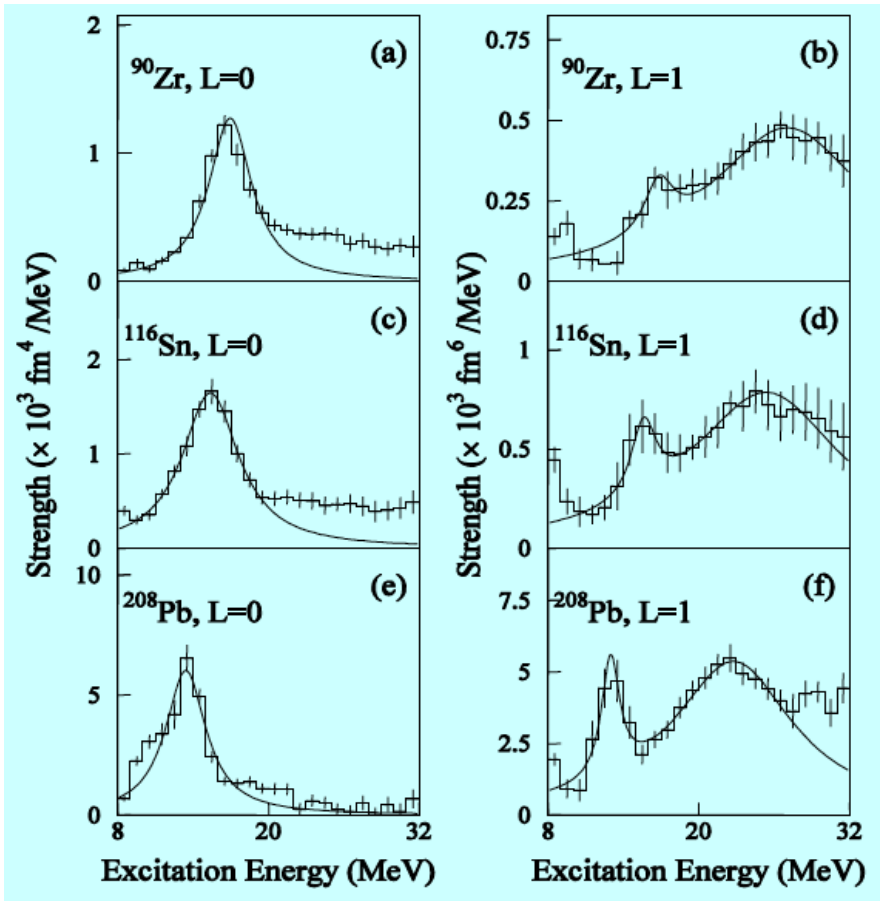

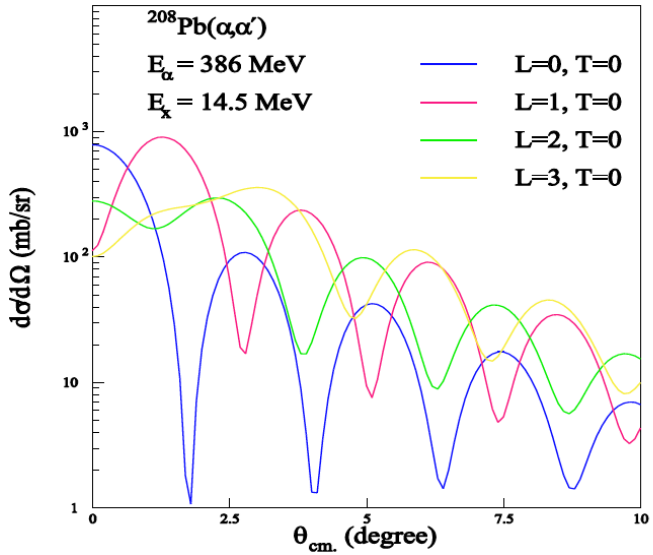

ISGMR, ISGDR

ISGQR, HEOR

100 % EWSR

At E_x= 14.5 MeV

E/A: binding energy per nucleon K_A: incompressibility

ρ : nuclear density

ρ_0 : nuclear density at saturation

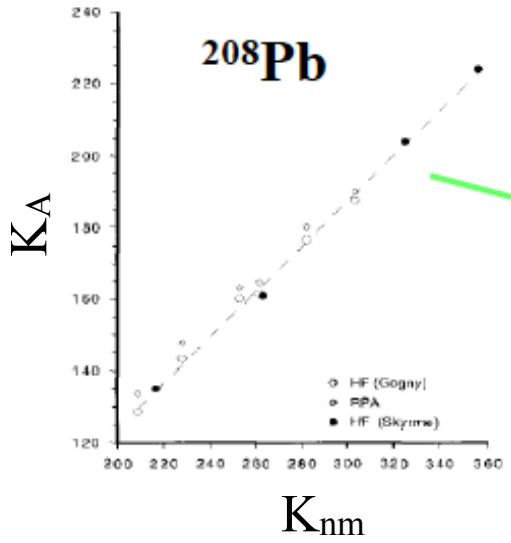

K_A is obtained from excitation energy of ISGMR

$K_A = 0.64 K_{nm} - 3.5$

J.P. Blaizot, NPA591 (1995) 435

From GMR data on ^{208}Pb and ^{90}Zr,

$K_\infty = 240 \pm 10$ MeV

[See, *e.g.*, G. Colò *et al.*, Phys. Rev. C 70 (2004) 024307]

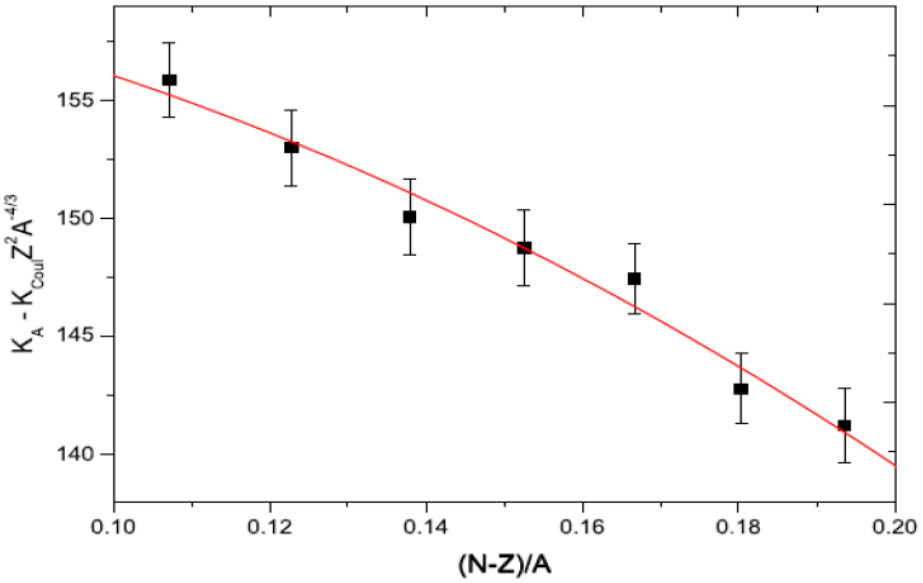

$$K_\tau = -550 \pm 100 \text{ MeV}$$

$$K_A \sim K_{vol}(1 + cA^{-1/3}) + K_\tau((N-Z)/A)^2 + K_{Coul} Z^2 A^{-4/3}$$

$$K_\tau^\infty = K_{\text{sym}} - 6L - \frac{Q_0}{K_\infty} L$$

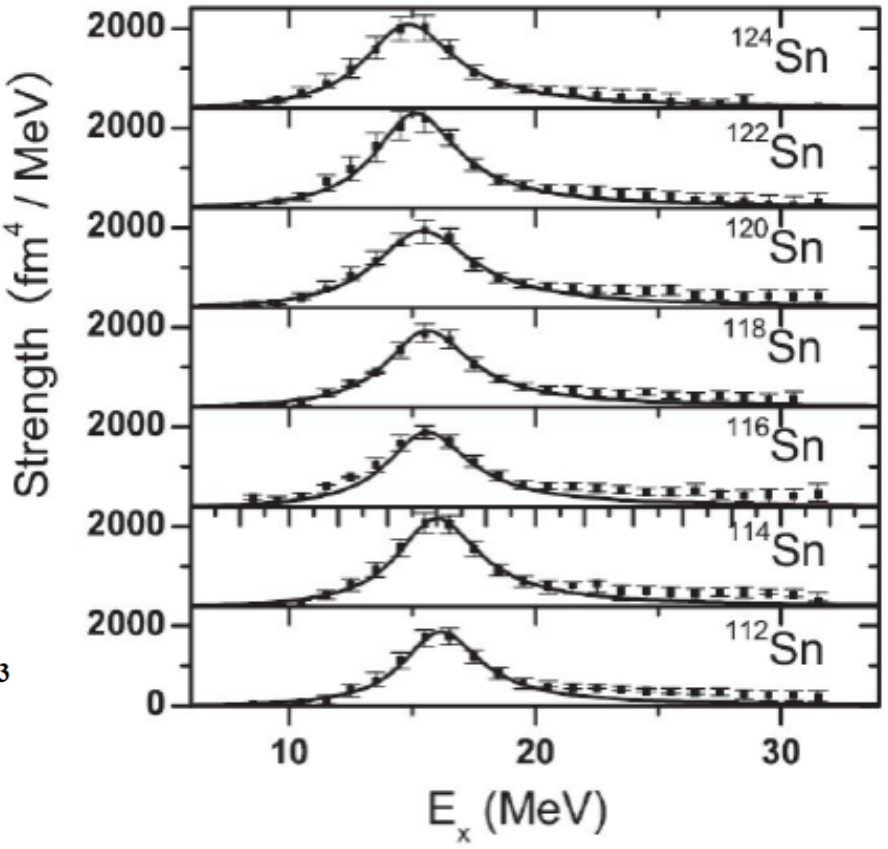

T. Li et al., PRC99, 162503(2007)

Softness of Sn and Cd nuclei is still unresolved

D. Patel et al., PLB**718**, 447 (2012)

Spin-M1 Responses
and
Quenching of IS/IV Spin-M1 Strengths

Spin-M1 SNME

H. Matsubara et al., PRL115, 102501 (2015)

- Summed up to **16 MeV**.
- Compared with shell-model predictions using the USD interaction

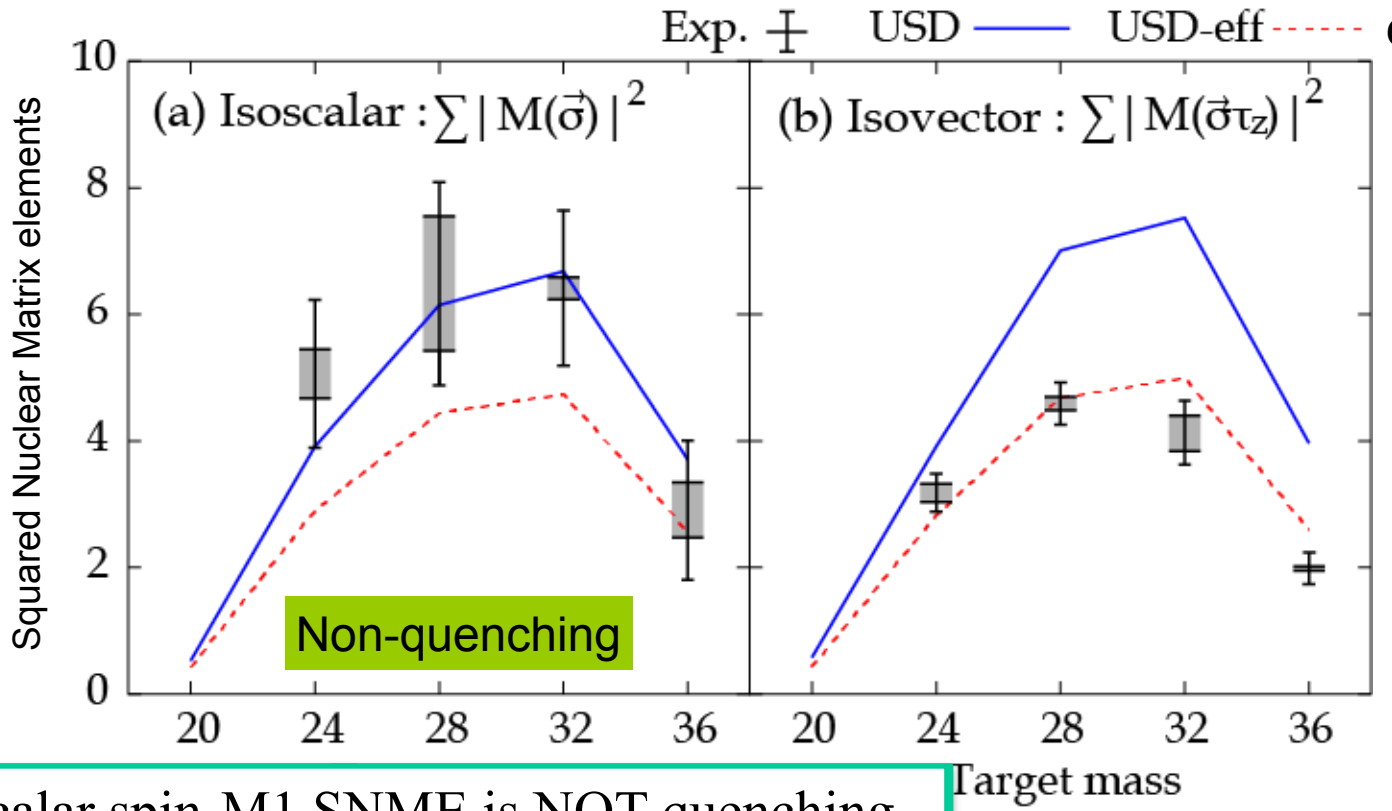

correction with $\frac{g^{eff}}{g^{bare}}$

Isoscalar spin-M1 SNME is NOT quenching.

It is important to understand more explicitly the quenching mechanism and the effect to the nuclearastrophysics

Spin Magnetic Susceptibility

Inversely energy-weighted sum rule of the spin-M1 strengths

$$\chi_\sigma^{spin} = \frac{8}{3N}\sum_f \frac{1}{\omega}\left|\langle f|\sum_i \boldsymbol{\sigma}_i|0\rangle\right|^2$$

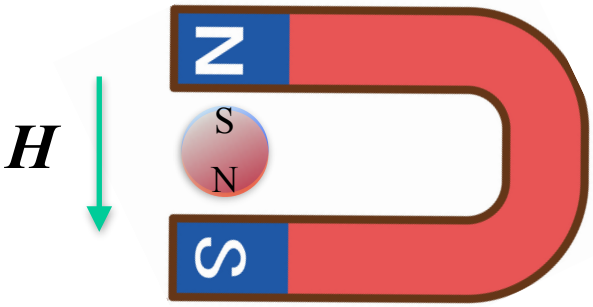

$$\mathbf{M} = \chi_\sigma \mathbf{H}$$

χ_σ: magnetic susceptibility

Spin Susceptibility of *N*=*Z* Nuclei

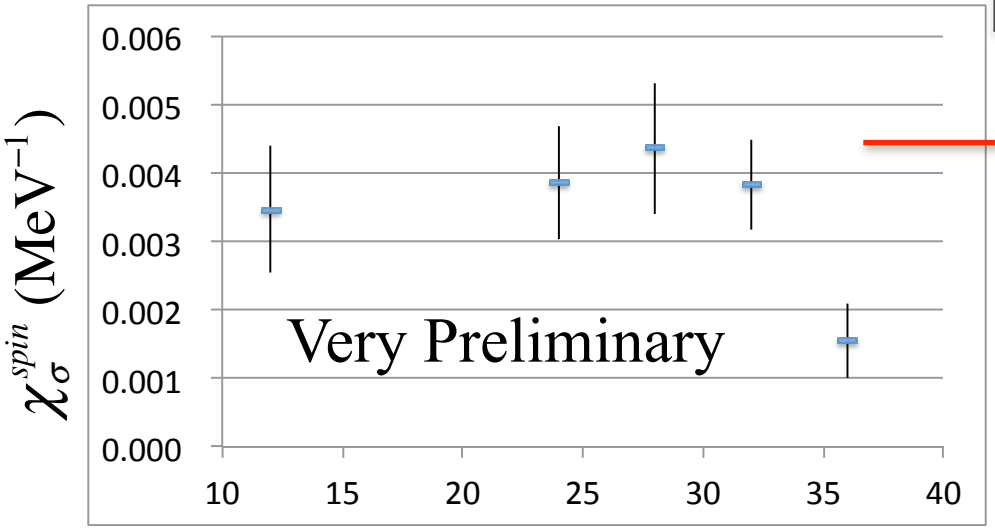

A

0.0044(7) MeV^{-1} at ρ=0.16 fm^{-3}

Neutron matter calc.
by AFDMC model

G. Shen et al., PRC**87**, 025802 (2013)

Further theoretical analysis is required.

Summary

- The **electric dipole polarizability** (EDP) of nuclei were measured. Constraints on the **symmetry energy parameters** were discussed at around the saturation density.

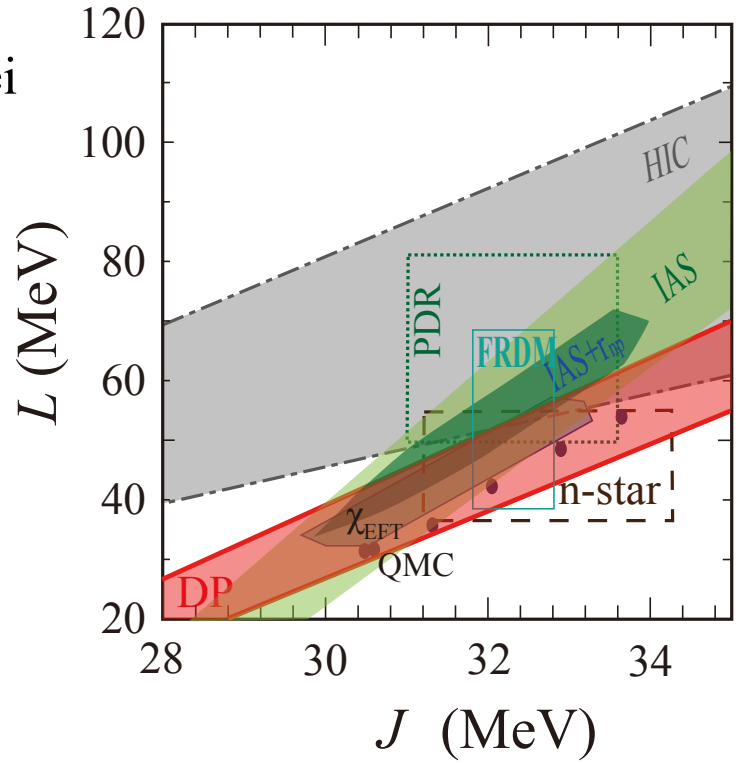

- Brief information on
  - nuclear incompressibility from GMR measurements
  - quenching of spin-M1 excitations, and spin susceptibility
  - alpha clusters on the nuclear surface

^{208}Pb RCNP-282 Collaboration

RCNP, Osaka University

A. Tamii, H. Matsubara, H. Fujita, K. Hatanaka,
H. Sakaguchi Y. Tameshige, M. Yosoi and J. Zenihiro

IKP, TU-Darmstadt

P. von Neumann-Cosel, A-M. Heilmann,
Y. Kalmykov, I. Poltoratska, V.Yu. Ponomarev,
A. Richter and J. Wambach

KVI, Univ. of Groningen

T. Adachi and L.A. Popescu

IFIC-CSIC, Univ. of Valencia

B. Rubio and A.B. Perez-Cerdan

Sch. of Science Univ. of Witwatersrand

J. Carter and H. Fujita

iThemba LABS

F.D. Smit

Texas A&M Commerce

C.A. Bertulani

GSI

E. Litivinova

Dep. of Phys., Osaka University

Y. Fujita

Dep. of Phys., Kyoto University

T. Kawabata

CNS, Univ. of Tokyo

K. Nakanishi,
Y. Shimizu and Y. Sasamoto

CYRIC, Tohoku University

M. Itoh and Y. Sakemi

Dep. of Phys., Kyushu University

M. Dozono

Dep. of Phys., Niigata University

Y. Shimbara

^{120}Sn RCNP-316 Collaboration

T. Hashimoto[†], A. M. Krumbholz[1], A. Tamii[2], P. von Neumann-Cosel[1], N. Aoi[2], O. Burda[2], J. Carter[3], M. Chernykh[2], M. Dozono[4], H. Fujita[2], Y. Fujita[2], K. Hatanaka[2], E. Ideguchi[2], N. T. Khai[5], C. Iwamoto[2], T. Kawabata[6], D. Martin[1], K. Miki[1], R. Neveling[7], H. J. Ong[2], I. Poltoratska[1], P.-G. Reinhard[8], A. Richter[1], F.D. Smit[6], H. Sakaguchi[2,4], Y. Shimbara[9], Y. Shimizu[4], T. Suzuki[2], M. Yosoi[1], J. Zenihiro[4], K. Zimmer[1]

[†]Institute for Basic Science, Korea
[1]IKP, Technische Universität Darmstadt, Germany
[2]RCNP, Osaka University, Japan
[3]Wits University, South Africa
[4]RIKEN, Japan
[5]Institute for Nuclear Science and Technology (INST), Vietnam
[6]Kyoto University, Japan
[7]iThemba LABs, South Africa
[8]Institut Theoretical Physik II, Universität Erlanen-Nürnberg, Germany
[9]CYRIC, Tohoku University, Japan

Collaboration ^{48}Ca

RCNP

TECHNISCHE UNIVERSITÄT DARMSTADT

Experiment: Darmstadt-Osaka
Theory: Darmstadt-Tennessee-TRIUMF

S. Bacca (TRIUMF)
S. Bassauer (TUD)
J. Birkhan (Darmstadt)
G. Hagen (ORNL)
H. Matsubara (RCNP)
M. Miorelli (TRIUMF)
P. von Neumann-Cosel (TUD)
T. Papenbrock (U Tennessee)
N. Pietralla (TUD)
A. Richter (TUD)
A. Schwenk (TUD)
A. Tamii (RCNP)